http://dx.doi.org/10.1097/mm9.0000000000000026

MedMat

Review

OPEN

High-entropy antibacterial materials

Peng-Wei Xue[a], Yu-Ling Chang[b], Chun Wang[a,c], Ge-Ting Sun[a, c], Rui-Ting Gao[d], Cheng-Yu He[a,*], Xiang-Hu Gao[a,c,*]

Abstract

High-entropy materials (HEMs), composed of 5 or more principal elements in near-equimolar ratios, have emerged as robust, multifunctional platforms for antimicrobial applications. This review introduces the fundamental principles and structural features of HEMs, focusing on their entropy-driven stability and synergistic properties. Four principal antibacterial mechanisms are discussed: controlled-release of biocidal metal ions, efficient photothermal sterilization, catalytic or oxide-mediated generation of reactive oxygen species, and electrostatic interactions resulting in contact killing. Representative studies illustrate how composition and microstructure can be engineered to optimize antimicrobial efficacy without sacrificing material integrity. The review then summarizes recent progress in applying high-entropy antibacterial materials across diverse areas, including biomedical implants and nanozymes for infection control and cancer therapy, self-disinfecting surfaces for public health, advanced catalysts for wastewater treatment, and antifouling, anticorrosion coatings for marine environments. Finally, current challenges, such as the complexity of compositional design and the need for comprehensive biosafety and environmental impact evaluation, are highlighted, alongside future directions involving computational design, multidisciplinary characterization, and scalable manufacturing. High-entropy antibacterial materials, thus, present a transformative strategy for addressing pathogenic threats, offering durable and broad-spectrum protection in a wide range of applications.

Keywords: Antibacterial mechanism, Biomedical applications, High-entropy materials, Photothermal sterilization, Robustness

1. Introduction

Materials have always been the backbone of civilization's progress, and the demand for advanced functional materials continues to grow. In recent years, especially after the COVID-19 pandemic in 2020, there has been a heightened awareness of public health and the need for effective antimicrobial materials[1,2]. The pandemic caused enormous loss of life and economic damage, and even after recovery, it left various long-term sequelae (e.g., psychological effects, fatigue, respiratory issues, and memory loss) and altered travel behavior[3–6]. These events underscored the importance of developing superior disinfection and antibacterial technologies. Bacterial infections remain pervasive threats in medicine, food safety, industry, and other fields[7–10]. However, many conventional disinfectants and antimicrobial agents have notable limitations. For example, alcohol-based disinfectants (e.g., ethanol) are highly flammable and potentially explosive[11,12]. Peroxide-based disinfectants are chemically unstable and can decompose quickly[13]. Chlorine-containing disinfectants cause secondary pollution due to residual chlorine; high chloride levels can harm ecosystems, human health, and corrode infrastructure (e.g., accelerating pipeline corrosion)[14,15]. These hazards, instability issues, and environmental concerns limit the applicability of traditional disinfectants. Consequently, there is an urgent need for new antimicrobial materials that overcome these drawbacks.

High-entropy materials (HEMs) have recently emerged as a promising class of materials to address this need. HEMs break the traditional paradigm of alloy design based on 1 or 2 primary elements[16–18]. Instead, HEMs are composed of multiple principal elements typically 5 or more in roughly equiatomic ratios that synergistically confer unique structures and properties[18]. By combining many elements, HEMs leverage cooperative "cocktail" effects that can be optimized to achieve superior performance. Indeed, many HEMs exhibit exceptional mechanical strength, hardness, thermal stability, corrosion resistance, and even radiation tolerance. These advantageous properties, along with their compositional flexibility, make these materials attractive for advanced applications, including as next-generation antimicrobial materials[19–28].

This review will discuss the fundamentals of HEMs, including their definition, classification, and key properties (Figure 1),

[a]*Key Laboratory of Energy Conservation and Energy Storage Materials of Gansu Province, Research Center for Resource Chemistry and Energy Materials, State Key Laboratory of Solid Lubrication, Lanzhou Institute of Chemical Physics, Chinese Academy of Sciences, Lanzhou, China,* [b]*Examination Centre of the First Affiliated Hospital of Shihezi University, Shihezi, China,* [c]*Center of Materials Science and Optoelectronics Engineering, University of Chinese Academy of Sciences, Beijing, China,* [d]*College of Chemistry and Chemical Engineering, Inner Mongolia Key Laboratory of Low Carbon Catalysis, Inner Mongolia University, Hohhot, China.*

**Corresponding authors: Address: Cheng-Yu He, Key Laboratory of Energy Conservation and Energy Storage Materials of Gansu Province, Research Center for Resource Chemistry and Energy Materials, State Key Laboratory of Solid Lubrication, Lanzhou Institute of Chemical Physics, Chinese Academy of Sciences, Lanzhou 730000, China. E-mail address: hechengyu@licp.cas.cn (C.-Y. He); Xiang-Hu Gao, Key Laboratory of Energy Conservation and Energy Storage Materials of Gansu Province, Research Center for Resource Chemistry and Energy Materials, State Key Laboratory of Solid Lubrication, Lanzhou Institute of Chemical Physics, Chinese Academy of Sciences, Lanzhou 730000, China. E-mail address: gaoxh@licp.cas.cn (X.-H. Gao).*

Peng-Wei Xue and Yu-Ling Chang contributed equally to this work.

MedMat (2026) 3:1

Copyright © 2025 The Authors. Published by Wolters Kluwer Health, Inc. This is an open access article distributed under the Creative Commons Attribution License 4.0 (CCBY), which permits unrestricted use, distribution, and reproduction in any medium, provided the original work is properly cited.

Received: 24 June 2025; Accepted 13 September 2025

Published online 29 September 2025

and examine the mechanisms by which these materials can inactivate microbes. We then survey recent progress in applying high-entropy antibacterial materials in areas such as biomedicine, public health, wastewater treatment, and marine environments. Finally, we outline the remaining challenges and prospects for the development and industrial deployment of high-entropy antibacterial materials.

2.Definition, classification, and properties of HEMs

2.1 Definition of HEMs

HEMs are defined by their multicomponent, near-equiatomic compositions: They contain 5 or more principal cations, each contributing roughly 5 to 35 at.% to the overall alloy or ceramic. This concept traces back to high-entropy alloys (HEAs) introduced by Yeh et al.[29] in 2004, which challenged the traditional paradigm of 1- or 2-element alloys. In a single-phase HEA, all constituent elements are uniformly distributed on one crystallographic lattice, typically face-centered cubic (FCC), body-centered cubic (BCC), or hexagonal close-packed (HCP), resulting in an extremely high configurational entropy (ΔS_{config})[29–35]. For an equimolar system,

$$S_{config} = -R(\sum_{i=1}^{M} x_i \ln x_i) \quad (1)$$

where M represents the number of elemental species, xi is the mole fraction of each component, and R is the universal gas constant (8.314 J mol^{-1} K^{-1}). Empirically, if $\Delta S_{\text{config}} \geq 1.5R$, the material is termed high-entropy (Figure 2A); between $1.0R$ and $1.5R$, it is medium-entropy; below $1.0R$, it is low-entropy[27,36,38]. Although this threshold is debated, especially for high-entropy oxides, where other thermodynamic factors play roles, it serves as a useful guideline for distinguishing true HEMs from conventional solid solutions[39–41].

This high entropy suppresses the formation of brittle intermetallics or complex compounds, stabilizing simple solid-solution phases over a broad temperature range. Importantly for antibacterial applications, the single-phase lattice ensures that biocidal ions (e.g., Cu, Ag, and Zn) are homogeneously integrated at the atomic scale. As a result, HEMs can provide controlled, long-term release of antimicrobial species without rapid depletion or phase segregation, enabling durable, self-sterilizing surfaces and coatings.

2.2 Classification of HEMs

Since their inception, HEMs have expanded into 2 major categories: HEAs and high-entropy ceramics. HEAs are multicomponent metallic alloys, often based on combinations of transition metals (e.g., Fe, Co, Ni, Cr, Mn, and Cu). As shown in

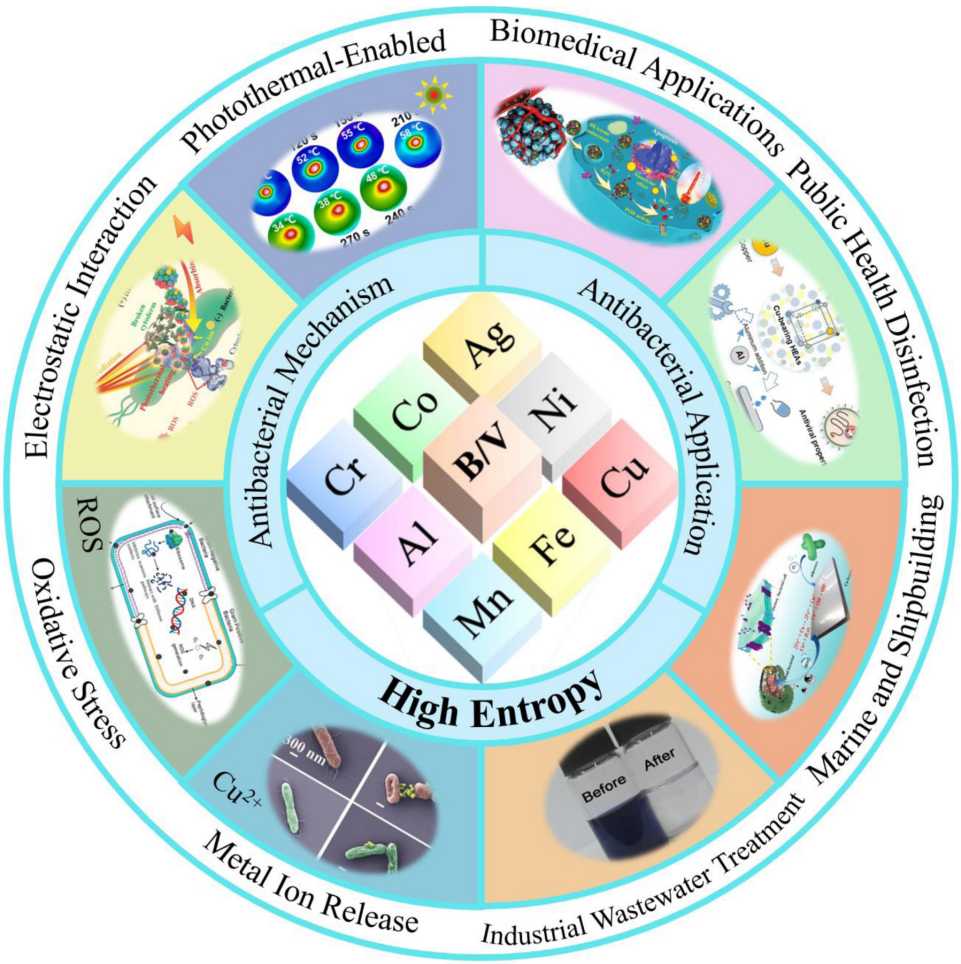

Figure 1. Graphical overview of the review.

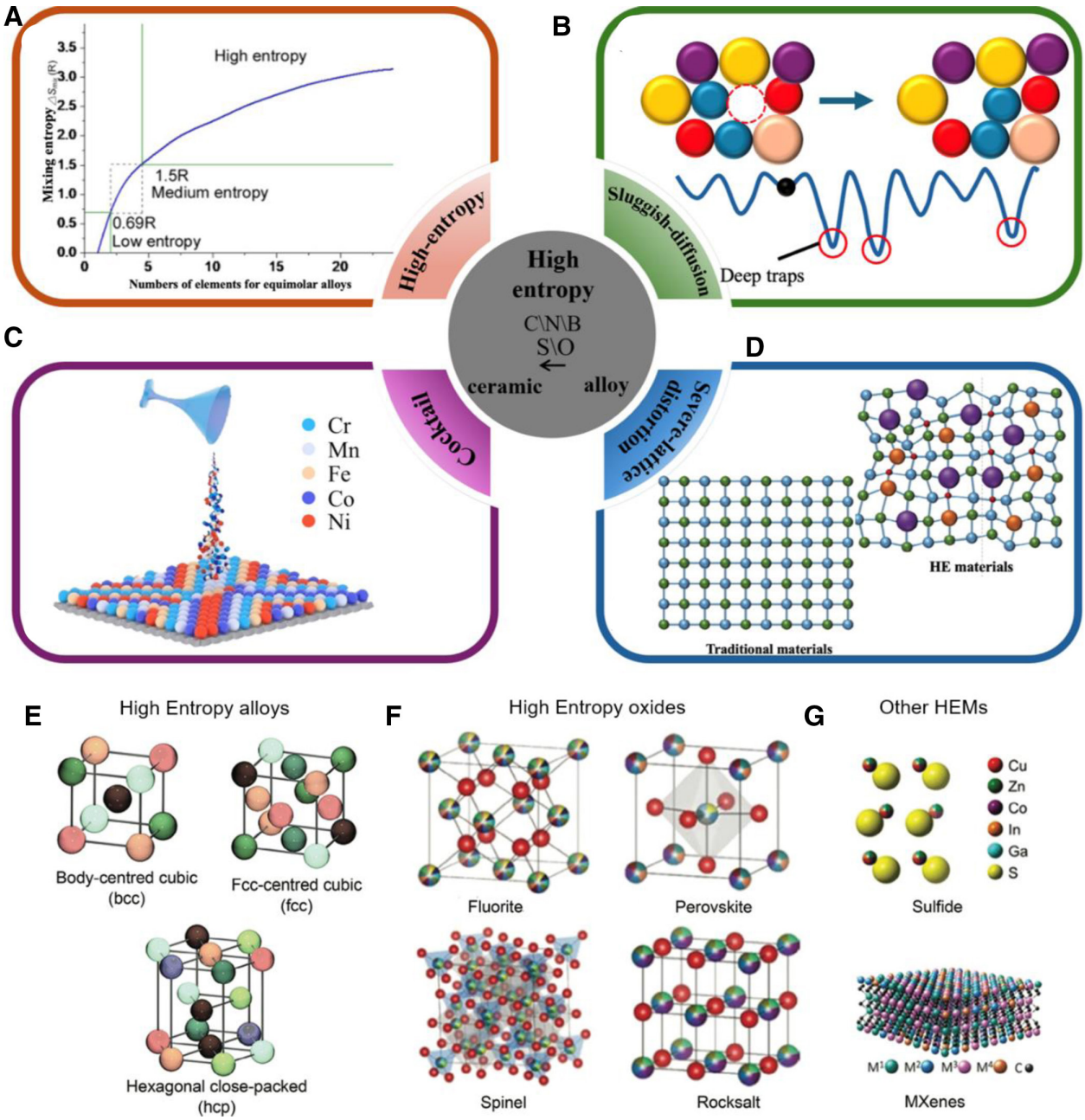

Figure 2. Schematic illustration of the principal effects and crystal structures in HEMs. (A) High-entropy effect: entropy-driven stabilization of single-phase solid solutions[36]. Copyright 2024 Elsevier Ltd. including those for text and data mining, AI training, and similar technologies. (B) Sluggish-diffusion effect: reduced atomic mobility in multicomponent lattices. (C) Cocktail effect: synergistic interactions among multiple elements yielding emergent properties[37]. Copyright 2023 Elsevier B.V. (D) Lattice-distortion effect: atomic-scale strain from size and bonding mismatches. (E) Representative crystal structures of high-entropy alloys: face-centered cubic (FCC), body-centered cubic (BCC), and hexagonal close-packed. (F) Common crystal structures of high-entropy oxides: spinel, perovskite, fluorite, and rock-salt. (G) Representative crystal structures of other HEMs[27]. Copyright 2024 Wiley-VCH GmbH.

Figure 2E, they adopt FCC, BCC, or HCP[42,43] lattices depending on elemental selection and processing conditions. Common synthesis routes include arc melting, induction melting, selective laser melting (SLM)[44], mechanical alloying, and thermal spraying. These techniques afford flexibility in shaping bulk components, coatings, or nanopowders. By incorporating biocidal elements such as Cu, Ag, or Zn into the HEA matrix, researchers have created antimicrobial HEAs that steadily release metal ions upon contact with moisture or biological fluids. For example, $Al_{0.4}$CoCrCuFeNi HEAs (AHEAs) release Cu^{2+} to inhibit biofilm formation by marine bacteria, while CoCrFeCuNi HEAs produced via SLM demonstrate nearly 100% kill rates for *Escherichia coli* and *Staphylococcus aureus* under both dark and illuminated conditions[45].

High-entropy ceramics include high-entropy oxides[46–49], nitrides[50,51], and carbides (Figure 2F)[52], each consisting of 5 or more metal cations in a single crystal lattice (e.g., spinel, perovskite, fluorite, and rock-salt structures)[53,54]. Techniques span solid-state reactions, sputtering, combustion synthesis, and in situ conversion of HEA substrates via oxidation or nitridation. High-entropy ceramic coatings exhibit outstanding hardness, chemical inertness, and thermal stability. When doped with Ag or Cu, they form robust, wear-resistant antimicrobial surfaces suitable for medical implants and industrial equipment

operating at elevated temperatures[55]. In addition, there are other types of HEMs, such as sulfides and MXenes (Figure 2G)[27].

2.3 Properties of HEMs

HEMs derive their superior performance from 4 interrelated core effects, each of which contributes directly to their multimodal antibacterial mechanisms. (1) High-entropy (entropy-stabilization) effect[56–58]: Large ΔS lowers the Gibbs free energy, favoring a single-phase solid solution. This stability ensures that antibacterial ions remain uniformly dispersed, enabling a steady, long-term release rather than a rapid burst that could lose efficacy or damage human cells. (2) Lattice-distortion effect[59]: Random atomic radii and bonding environments produce local lattice strains, leading to nanoscale surface roughness (Figure 2D). Such rough, distorted topographies can mechanically disrupt bacterial membranes upon contact, complementing chemical biocidal actions. (3) Complex multielement matrices impede atomic mobility, reducing diffusion coefficients (Figure 2B)[60–62]. This "sluggish diffusion" slows down the leaching of metal ions, which translates into prolonged ion-release profiles and sustained antimicrobial activity over weeks to months. (4) Cocktail (synergy) effect: Interactions among multiple elements generate emergent properties that exceed those of individual components (Figure 2C)[37,63,64]. In an antibacterial context, the cocktail effect enables cooperative mechanisms: Cu^{2+} and Ag^{+} ion release, photothermal heating under light exposure (via Ni/Co/Cu electronic transitions), and catalytic generation of reactive oxygen species (ROS) from hydrogen peroxide (H_2O_2). For instance, FeMnCoTiVCu HEA nanoparticles can simultaneously heat to 80 °C under solar illumination and release Cu^{2+}, achieving >99% bacterial kill rates within minutes[65].

Together, these 4 effects provide the structural and physicochemical foundation for robust, multipronged antimicrobial action. Their compositional tunability enables precise control over ion-release kinetics, optical absorption, and catalytic pathways, positioning HEMs as a versatile platform for next-generation antibacterial technologies in self-sterilizing implants, healthcare surfaces, light-activated coatings, and nanozyme therapies.

3. Antibacterial mechanisms of HEMs

When imbued with antimicrobial functionality, HEMs offer new pathways for killing or inhibiting microorganisms. The antibacterial mechanisms of HEMs generally derive from the presence of bioactive metal elements and the unique physicochemical effects of the high-entropy matrix. Four primary bactericidal mechanisms have been identified in high-entropy antimicrobial materials: Metal ion release, photothermal heating, oxidative stress induction, and electrostatic interaction. These can act individually or synergistically to achieve sterilization. We discuss each mechanism below.

3.1 Metal ion-release mechanism

One straightforward strategy to endow an alloy with antibacterial activity is to incorporate known antimicrobial metal elements into its composition so that the alloy gradually releases metal ions in situ. This approach has long been used in traditional alloys: For example, embedding copper, silver, or zinc into stainless steel (SS), titanium, or magnesium alloys to create antibacterial surfaces[66]. Copper (Cu^{2+}), silver (Ag^{+}), and zinc (Zn^{2+}) ions are well-established for their strong bactericidal effects[67–69]. In such Cu/Ag/Zn-doped alloys, the metal ions will slowly leach out from the surface when in contact with moisture or biological fluids, and these ions can then interact with bacteria or viruses to inactivate them.

Taking silver as an example: Ag^{+} ions released from a surface tend to accumulate on bacterial cell membranes, disrupting membrane integrity and causing cell inactivation. Additionally, silver ions can penetrate cells and induce the generation of ROS inside the bacteria, leading to oxidative damage and cell death[25]. These 2 effects, including membrane disruption and intracellular oxidative stress, are the primary modes of silver's antimicrobial action. Copper and zinc ions have similarly been reported to damage bacterial membranes and interfere with cellular metabolism[67–69]. While the release of metal ions is effective for disinfection, the rate and concentration of ion release are critical to antimicrobial efficacy[70–72]. Too slow a release may be insufficient to kill microbes, whereas too rapid or excessive release could be toxic to human cells or the environment. Thus, controlling the ion-release kinetics is important in alloy design. Ozdemir et al.[55] deposited Ag coatings on HEAs $Ti_{23}Ta_{10}Hf_{27}Nb_{12}Zr_{29}$ and $Ti_{23}Ta_{10}Hf_{27}Nb_{12}Zr_{29}$ using magnetron sputtering, thereby enhancing antibacterial activity. By tuning deposition time and Ar flow rate, they modulated the coating microstructure and controlled Ag^{+} release. Lower Ar flow produced finer Ag nanoparticles and rougher surfaces, accelerating ion release, whereas increased sputtering time thickened the coating and strengthened the (111) orientation, which suppressed Ag^{+} dissolution. At a 40-min deposition (≈350 nm thickness), the (111) texture was maximized and Ag^{+} release minimized, demonstrating that microstructural engineering enables kinetic control of antibacterial ion release.

In contrast, traditional copper-bearing SS or other antimicrobial alloys often require complex processing (such as specialized heat treatments) to incorporate the bioactive element and achieve a sustained release. Moreover, introducing these elements can sometimes degrade the base alloy's chemical or mechanical properties. For instance, adding copper to SS can alter its corrosion behavior and microstructure, sometimes necessitating careful trade-offs[73,74].

In contrast, HEAs offer a more flexible platform for ion-based antimicrobial design. HEAs intrinsically possess excellent mechanical strength and hardness, stable structures, and superior corrosion and oxidation resistance[75–77]. They can also be produced in bulk with conventional processes[78], which simplifies fabrication. By substituting a fraction of the HEA's components with antimicrobial elements (Cu, Ag, Zn, etc.), one can create a high-entropy antibacterial alloy that slowly releases biocidal ions without the extensive processing or property degradation that plagues traditional alloys. The high-entropy matrix, with its uniform multielement distribution, can facilitate a more even release of ions and maintain overall alloy performance.

Thanks to these advantages, high-entropy antibacterial alloys have fewer limitations and broader application prospects compared with conventional antimicrobial alloys. For example, Zhou et al.[79] designed a novel AHEA by vacuum induction melting that incorporated copper as an antibacterial element (Figure 3A). This HEA was shown to release a high concentration of Cu^{2+} ions, effectively inhibiting the growth of highly corrosive marine bacteria and preventing biofilm formation (Figure 3B, C). In antibacterial tests, the HEA sample was compared with 304 SS, Cu-containing 304 SS (with 4.1 wt% Cu), and pure copper, using standard plate-count methods. The HEA achieved

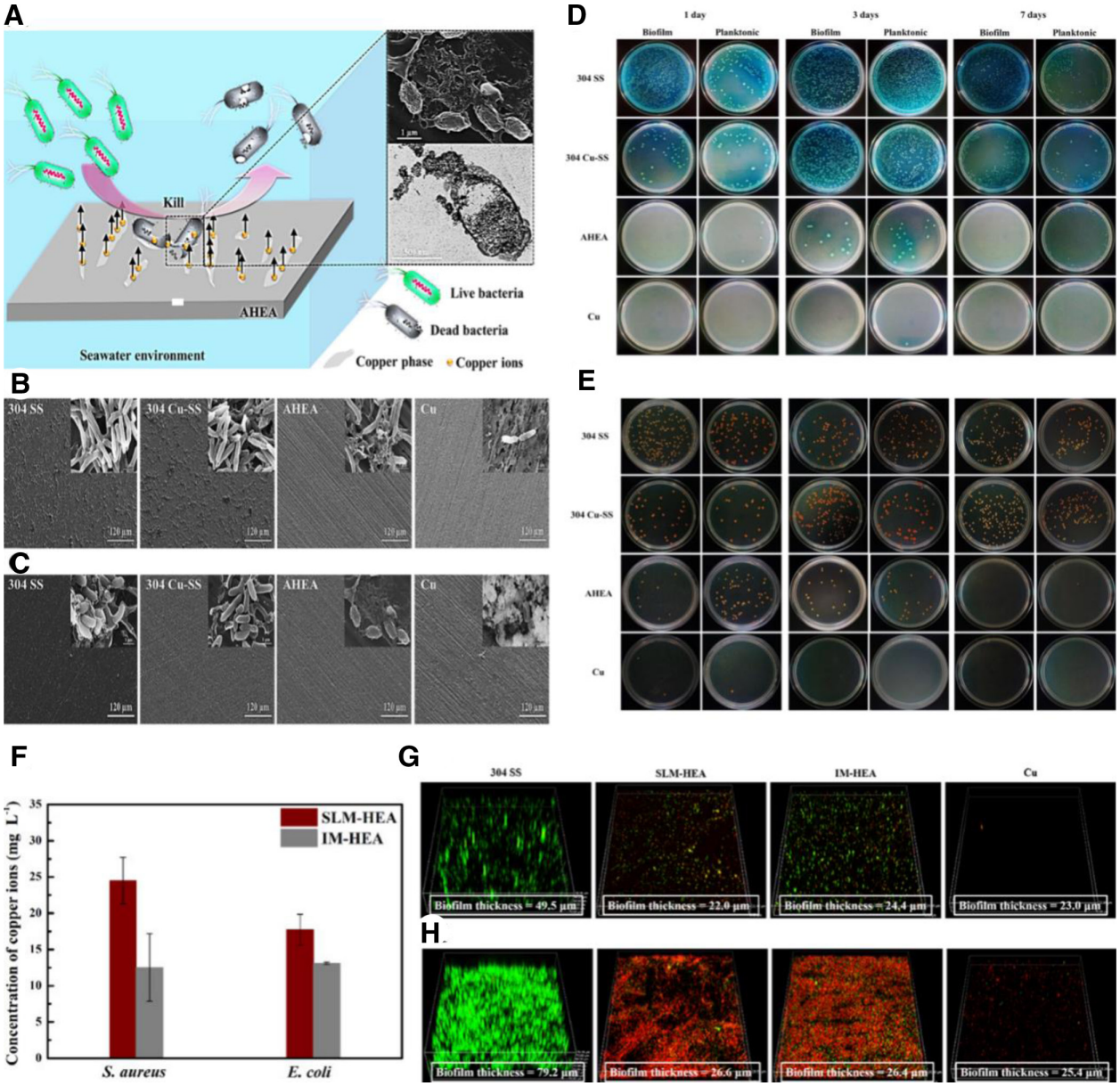

Figure 3. Antimicrobial evaluation of HEA coupons. (A) Schematic illustrating the antibacterial mechanism of activated HEA coupons: bacterial adhesion, Cu^{2+} release, and cell inactivation. (B, C) Representative photographs of Pseudomonas aeruginosa (B) and Burkholderia vietnamensis (C) colonies on 304 SS, 304-Cu SS, AHEA, and pure Cu coupons after 7 days. (D, E) Quantification of coupon-associated biofilm (D) and planktonic cells (E) on 2216E agar at 1, 3, and 7 days for P aeruginosa and B vietnamensis[79]. Copyright 2020 Elsevier. (F) Cu^{2+} concentration released from selective-laser-melting (SLM) HEA versus in situ-alloyed (IM) HEA after 24 h in bacterial suspension. (G, H) Live/dead staining of bacterial attachment on coupon surfaces of (G) S aureus and (H) E coli after incubation with 304 SS, SLM-HEA, IM-HEA, and Cu for 24 h. Green fluorescence represents living cells, while red fluorescence represents dead cells[56]. Copyright 2022 Elsevier.

dramatically fewer bacterial colonies than 304 SS or the Cu-alloyed 304 SS after exposure to Gram-negative and Gram-positive marine bacteria. In fact, the HEA's antibacterial efficacy was nearly equivalent to pure copper: It achieved ~100% killing of Gram-negative bacteria and ~99.99% killing of Gram-positive bacteria within 7 days, whereas the Cu-bearing 304 SS showed no significant antibacterial effect (Figure 3D, E)[79]. The HEA, thus, provided broad-spectrum, long-lasting antibacterial performance approaching that of pure copper, yet in a much more durable alloy form.

Different processing routes for the HEA can also influence ion release and antibacterial outcomes. Gao et al.[56] prepared the CoCrFeCuNi high-entropy antibacterial alloy by 2 methods: SLM and conventional induction melting (in situ alloying). Then, they compared it with the alloy obtained by traditional metallurgical methods to observe its antibacterial properties. The SLM-fabricated HEA had a more homogeneous microstructure with uniformly distributed Cu, leading to a higher and more consistent release of Cu^{2+} ions (Figure 3F). As a result, the SLM-HEA exhibited superior antibacterial performance. Therefore, the HEAs produced through SLM exhibit outstanding antibacterial properties. The bacterial killing rate of SLM samples is approximately 98% (*E coli*) and over 99% (*S aureus*), significantly better than that of the cast version. Then, the bacterial attachment was visually demonstrated through the live/dead chromosome technique. As shown in Figure 3G, H, SLM-HEA not only has good antibacterial activity against *S aureus*, but also performs well in inhibiting the formation of *E coli* biofilms.

SLM-HEA inhibits bacterial growth and biofilm formation more effectively than cast HEA[56].

3.2 Photothermal-enabled antibacterial mechanism

HEMs can also serve as potent photothermal agents. Photothermal disinfection relies on materials that absorb light (often in the near-infrared or broadband solar spectrum) and efficiently convert it into heat, thereby raising the local temperature enough to kill microorganisms. Many HEMs have excellent photothermal conversion capabilities[80]. By tailoring their composition, one can adjust their electronic structure (e.g., bandgap and plasmonic response) to broaden light absorption across a wide range of wavelengths[81]. In principle, an ideal photothermal material would absorb the entire solar spectrum and rapidly convert that energy to heat, producing a localized high-temperature effect that destroys bacteria and viruses upon light irradiation[82,83].

High-entropy nanoparticles exhibit broadband light harvesting via both localized surface plasmon resonance (LSPR) and band-to-band transitions. LSPR enhances photon–electron coupling and nonradiative decay into heat, whereas subbandgap defect states and entropy-narrowed bandgaps facilitate electron–hole generation and phonon-mediated thermalization. Entropy-enabled defect chemistry and multielement d-states thus deliver efficient, rapid photothermal conversion alongside structural robustness under repeated cycles. Compared with typical 2D photothermal agents, HEMs uniquely combine durable photothermal heating with synergistic bactericidal routes (controlled ion release, ROS catalysis, and contact killing), enabling higher sustained efficacy under complex media[27,84,85].

In contrast, many traditional photothermal materials exhibit notable limitations. For example, graphene oxide suffers from poor dispersion stability, leading to sedimentation during storage and loss of active sites. Its weak near-infrared absorption also results in low photothermal efficiency, and the absence of antibacterial ion release further reduces its bactericidal performance[86]. Similarly, MoS_2 nanosheets with enzyme-mimetic activity rely mainly on catalytically active edge sites. However, conventional synthesis routes preferentially expose thermodynamically stable (002) basal planes rather than active edges, which drastically limits catalytic efficiency. Moreover, effective sterilization requires not only ROS generation but also efficient bacterial capture. The intrinsically smooth surface of pristine MoS_2 lacks nanoscale roughness, making it difficult to trap bacteria and thereby lowering its antibacterial efficacy[87]. Taken together, these comparisons highlight how the intrinsic features of HEMs, such as configurational entropy, defect-assisted light absorption, and synergistic multimechanistic actions, address the shortcomings of conventional photothermal agents, positioning HEMs as highly promising candidates for robust, broad-spectrum photothermal antibacterial applications.

Beyond intrinsic optical advantages, HEAs also allow compositional tuning of electronic states. By adjusting the elemental ratios, d-band states, and interband transition probabilities can be engineered to optimize light absorption (Figure 4A)[81]. Li et al.[81] demonstrated this by designing FeCoNiTiVCrCu HEA nanoparticles, which exhibited an average absorbance exceeding 96% across the solar spectrum. Remarkably, only 100 mg of these nanoparticles could be heated from 0 to ~80 °C within 60 seconds under one-sun illumination (Figure 4B), and cooled rapidly upon removal of light. Such a rapid and efficient photothermal response highlights the promise of HEAs for solar-driven sterilization and related applications.

Another example is provided by An et al.[65], who synthesized a series of FeMnCo-based HEA powders and investigated their photothermal antibacterial efficacy. One of their HEA compositions, FeMnCoTiV, achieved a solar absorption rate of 85.6% over the 200 to 2500 nm wavelength range (Figure 4C), indicating excellent broadband absorption. Upon illumination with a 300 W xenon-lamp for 60 minutes, the HEA powders exhibited significantly enhanced bactericidal activity against both *E coli* and *S aureus* compared with dark conditions (Figure 4D, E). For simpler compositions without Cu (e.g., FeMnCoNi or FeMnCoTiV), the antibacterial rate in the dark was relatively low (Figure 4E), but under light exposure, these reached >80% (for *E coli*) and >74% (for *S aureus*) killing[65]. Notably, HEA compositions containing Cu (FeMnCoTiVCu and FeMnCoTiVCrNiCu) achieved nearly 100% bacterial elimination even in the absence of light, thanks to Cu ion release, and maintained ~100% kill under illumination as well[65]. As shown in Figure 4F, the presence of Cu in these HEAs not only provides an ion-release mechanism but also may enhance photothermal conversion (as Cu can contribute plasmonic effects). Additionally, the researchers observed that light exposure accelerated the release of Cu^{2+} from the HEA, further boosting the antibacterial effect[88]. Thus, the photothermal mechanism in HEAs can work synergistically with ion release: Light-generated heat damages and directly kills microbes, while simultaneously promoting the leaching of antibacterial metal ions, leading to a combined bactericidal effect.

Photothermal HEMs are particularly attractive for on-demand disinfection applications. Surfaces or particles made of such materials can remain inert under normal conditions, but upon exposure to a suitable light source (solar or laser), they rapidly heat to sterilize their environment. This approach has been suggested as a way to create self-sterilizing surfaces in healthcare or to develop light-activated antibacterial treatments that do not rely on chemical biocides[89].

3.3 Oxidative stress (ROS generation) mechanism

HEAs containing oxide-forming elements can generate ROS that kill bacteria via oxidative stress. Many HEAs readily form a thin oxide film on their surface when exposed to air. This surface oxide can have intrinsic oxidizing properties. When bacteria come into contact with such an oxidized HEA surface, it can trigger the production of ROS and oxidative damage within the bacterial cells. Common ROS include superoxide anions ($\cdot O_2^-$), hydroxyl radicals ($\cdot OH$), and singlet oxygen ($^1O_2$). These species are highly reactive and can attack vital cellular components, thereby damaging lipid membranes, proteins, and DNA. For instance, superoxide and hydroxyl radicals can peroxidize unsaturated fatty acids in the bacterial cell membrane, compromising membrane integrity and causing leakage of cellular contents[90]. ROS can also oxidize enzymes and nucleic acids inside the cell, inactivating metabolic processes and leading to cell death.

In HEMs, the generation of ROS is often reinforced by the coexistence of multiple redox-active metal ions within their oxide layers. For instance, Wang et al.[91] synthesized a high-entropy 2-dimensional layered double hydroxide (Co, Cu, Fe, Zn, Al), which released these ions sequentially to achieve therapeutic effects against tumor cells. Specifically, Co^{2+}, Fe^{3+}, and Cu^{2+} exhibited superoxide dismutase-, peroxidase-, and glutathione peroxidase (POD)-like activities, respectively. Through these enzyme-mimicking reactions, tumor metabolites were continuously converted into cytotoxic ROS. Under acidic conditions, Co^{2+} transformed $\cdot O_2^-$ into H_2O_2, Fe^{3+} catalyzed the Fenton-like

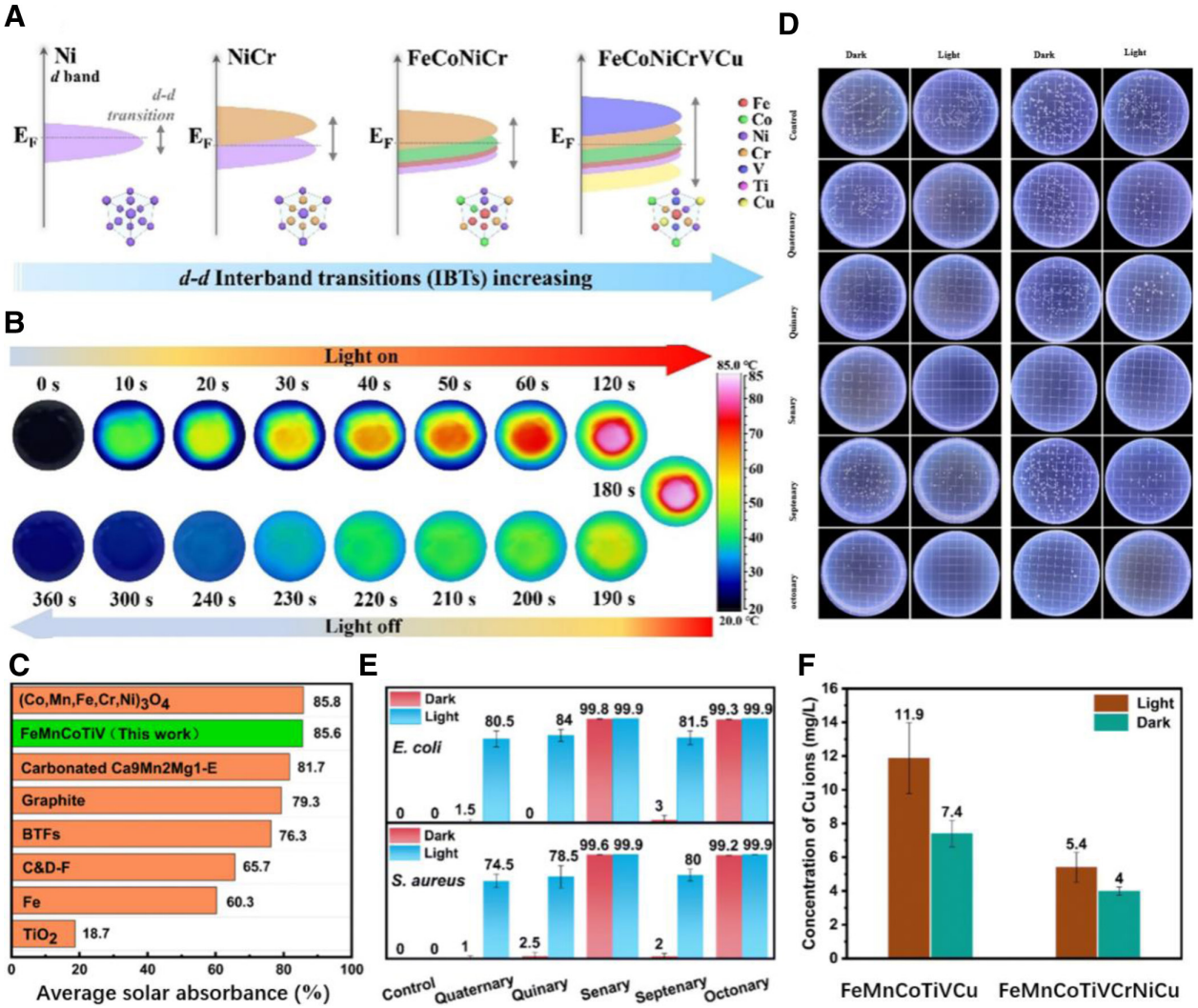

Figure 4. Photothermal properties and antibacterial performance of HEMs. (A) HEAs with schematic depictions of d-band electron filling by various 3d transition metals. (B) Photothermal heating of septenary HEA nanopowder (100 mg) under one-sun illumination for 180 s, followed by rapid cooling upon light removal[81]. Copyright 2021 Wiley-VCH GmbH. (C) Average solar-spectrum absorption of the HEA powders across the full 300 to 2500 nm range. (D) Photographs of E coli and S aureus colonies after 60-min exposure to 5 High-Entropy Nanoparticles (HENP)s compositions–quaternary (FeMnCoNi), quinary (FeMnCoTiV), senary (FeMnCoTiVCu), septenary (FeMnCoTiVCrNiCu), and octonary (FeMnCoTiVCrNiCuZn)-under both dark (no light) and 300 W xenon-lamp illumination conditions. (E) Quantified antibacterial rates of each high-entropy alloy powders composition against E coli and S aureus under light exposure and in the dark. (F) Concentrations of Cu^{2+} ions released from FeMnCoTiVCu and FeMnCoTiVCrNiCu HENPs into bacterial suspensions after 24 h at 37 °C[65]. Copyright 2025 Royal Society of Chemistry.

conversion of H_2O_2 into ·OH radicals, while Cu^{2+} consumed glutathione and further amplified oxidative stress.

The high-entropy effect not only improves the thermodynamic stability of these nanomaterials but also suppresses nanoparticle aggregation due to sluggish diffusion and lattice distortion. As a result, subnanometer particle sizes can be preserved, providing large specific surface areas and dense active sites, which significantly enhance catalytic performance. Another example is provided by Ai et al.[93], who synthesized subnanometer RuRhPtIrMo high-entropy nanozymes. These materials adsorbed H_2O_2 strongly (DFT adsorption energy: −0.726 eV), stabilizing it on the surface as H_2O_2*. The O–O bond was then stretched and activated into a transition state, eventually cleaving to form ·OH radicals under electron transfer. This ROS generation endowed the nanozymes with potent cytotoxicity toward tumor cells. Similarly, Grisales et al.[90] demonstrated this with a silver-doped high-entropy nitride coating, $(TiTaZrNbN)_{1-}xAgx$, which gradually releases Ag^+ ions and also generates ROS (·OH and $\cdot O_2^-$) upon exposure to moisture (Figure 5B). They deposited this $(TiTaZrNbN)_{1-}xAgx$ coating on steel via magnetron sputtering, with varying silver content (Figure 5C). In antibacterial assays, all Ag-containing HEA coatings showed clear inhibition zones against *Pseudomonas aeruginosa* (a Gram-negative bacterium), whereas an uncoated steel control showed no inhibition zone[90]. The coatings also exhibited antiviral activity. Mechanistic analysis (Figure 5A) indicated that the coating releases Ag^+ as well as ROS such as ·OH and $\cdot O_2^-$ from the oxidized silver nanoparticles in the matrix. These species work together to inhibit bacterial growth: Ag^+ disrupts cell structures and ROS induces oxidative damage, together producing a significant bactericidal effect.

Another compelling example is the use of HEAs as nanozymes, which are nanomaterial-based enzyme mimics. Yang et al.[92] developed a PdMoPtCoNi high-entropy nanozyme that exhibits POD-like catalytic activity (Figure 5D). Figure 5E, F shows the Michaelis-Menten curves of HEA NWs and PdMoPt for different concentrations of tetramethylbenzidine (TMB) and

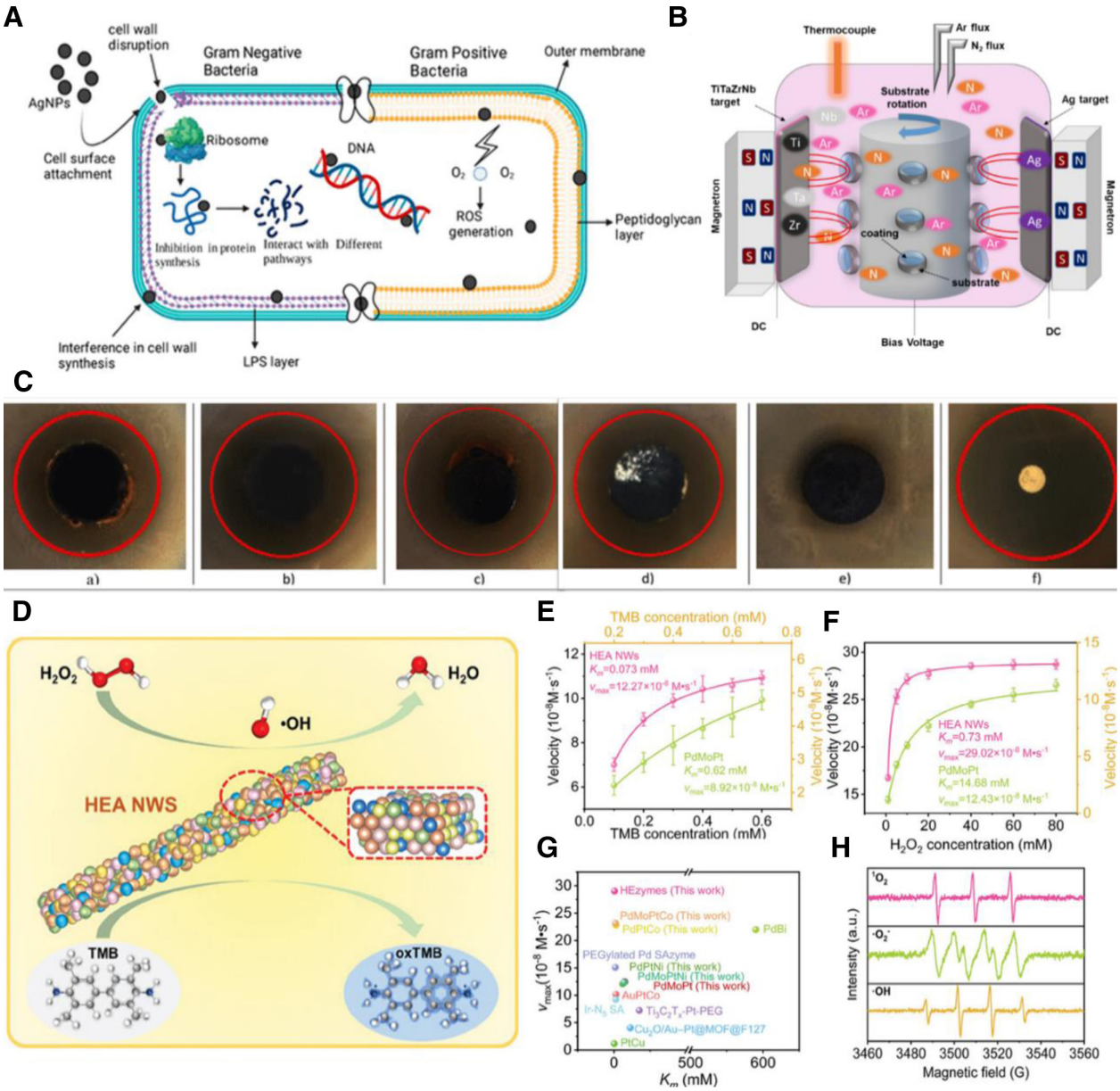

Figure 5. Antibacterial activity and catalytic mechanisms of silver-doped HEMs. (A) Schematic comparison of how Ag nanoparticles interact with Gram-negative and Gram-positive bacterial cell envelopes, illustrating differences in membrane affinity and disruption pathways. (B) Schematic of the vacuum chamber used for the fabrication of the silver-doped high-entropy coatings. (C) Photographs of inhibition zones for Pseudomonas aeruginosa on (TiTaZrNbN)Ag_x coatings deposited at different sputtering powers: RN-50 W, RN-70 W, RN-90 W, and RN-110 W; uncoated steel; and a ciprofloxacin-loaded filter paper positive control[90]. Copyright 2025 American Chemical Society. (D) Schematic illustration of the POD-like catalytic process of the HEA NWs. The yellow axes are the parameters corresponding to PdMoPt. Michaelis-Menten curve of the HEA NWs and PdMoPt toward different concentrations of (E) TMB and (F) H_2O_2, respectively. (G) Comparison of Km and vmax of PdMoPtCoNi HEzymes with other reported catalysts using H_2O_2 as substrate. (H) Electron spin resonance (ESR) spectra confirming the formation of hydroxyl (·OH), superoxide ($\cdot O_2^-$), and singlet oxygen ($^1O_2$) radicals during the catalytic cycle[92]. Copyright 2024 The Author(s).

H_2O_2. It can be seen from the figures that HEA NWs exhibit superior POD-like activity in catalytic reactions and efficiently catalyze the decomposition of H_2O_2 into ROS such as ·OH, $\cdot O_2^-$, and $^1O_2$ (Figure 5H)[92]. Compared with other alloy nanozymes (PdMoPt, PdPtCo), they show a stronger affinity for TMB and H_2O_2, and the maximum reaction rate of HENPs is relatively higher, indicating their better catalytic performance (Figure 5G). When the high-entropy nanocatalyst is compared with the reported catalysts, it is a highly promising POD mimic due to its excellent catalytic efficiency and ideal affinity. When tested with a chromogenic substrate (TMB, 3,3′,5,5′-tetramethylbenzidine), the HEA nanozyme produced a color change indicative of robust catalytic generation of ROS, even under harsh conditions. In a biological context, such a nanozyme can continuously produce ROS that kill bacteria (or cancer cells, in therapeutic applications) and can be recycled and reused, making it a cost-effective and durable alternative to natural enzymes[92]. The high catalytic efficiency and strong substrate affinity are attributed to the multiple active metal sites and synergistic d-electron interactions in the HEA structure. This work highlights a future direction where HEMs serve as catalytic antibacterial agents, converting benign precursors (such as H_2O_2, which may be present in immune responses or added externally) into a barrage of ROS that eradicate pathogens.

3.4 Electrostatic interaction and contact-killing mechanism

Finally, high-entropy antibacterial materials can exploit electrostatic interactions to capture and kill bacteria. Bacterial cell surfaces (especially for Gram bacteria) are typically negatively charged at neutral pH, due to the presence of anionic groups in lipopolysaccharides and peptidoglycan on their cell walls. This negative charge enables strong electrostatic attraction to positively charged HEMs, facilitating intimate contact at the cell–material interface. Such close interactions promote membrane disruption and can be further reinforced by the localized release of antibacterial ions. The key structural difference lies in the outer membrane[94,95], which is unique to Gram-negative bacteria, whereas Gram-positive bacteria rely on a thick peptidoglycan layer.

This distinction influences permeability and binding: Gram-positive bacteria often provide more accessible binding sites for cationic HEMs, while the outer membrane of Gram-negative bacteria can serve as a selective barrier that modulates electrostatic interactions and penetration efficiency. These contrasting features highlight how bacterial surface properties critically regulate the efficacy of HEM-induced contact killing[98,99]. In contrast, certain metals within HEAs can undergo polarization or partial ionization at the surface, imparting a net positive charge to the nanoparticles or their surface oxides. The resulting electrostatic attraction between positively charged alloy surfaces and negatively charged bacterial membranes promotes close contact, membrane disruption, and ultimately bacterial inactivation.

In HEAs containing elements such as Fe, Ni, and Ti, the surface can develop a positive charge as these metal atoms oxidize or polarize in solution. This creates an electrostatic attraction between the HEA surface (positive) and the bacteria (negative). This mechanism essentially brings bacteria into close contact with the material. Hua et al.[96] illustrated this concept by using model polystyrene nanoplastics with different charges. They prepared positively charged, neutral, and negatively charged nanopolymers and studied their interaction with *E coli* and *Bacillus subtilis*, as shown in Figure 6A. The positively charged nanoparticles strongly adhered to the bacterial membranes and even penetrated into the cells, accumulating and eventually causing cell lysis, whereas neutral and negatively charged particles showed minimal cell entry or disruption. This confirms that positively charged surfaces/particles can markedly reduce bacterial viability by concentrating at the cell surface and facilitating other lethal interactions[100].

HEAs can be designed to leverage this electrostatic attraction and also incorporate a contact-killing surface topology. Many HEA surfaces are inherently rough or can be engineered to have nano- or microscale protrusions (due to solidification microstructure or deliberate surface treatment). These sharp edges or spikes can physically pierce bacterial membranes upon contact, leading to cell rupture. If the HEA carries a positive charge, it will actively draw bacteria toward it, and the nanospikes on the surface can puncture the cell envelope. For example, Li et al.[97] synthesized an HEA FeNiTiCrMnCu that develops a slight positive surface charge in physiological conditions. They observed that this HEA's positively charged nanoparticles would gravitate toward negatively charged bacterial membranes by electrostatic attraction. Upon contact, the nanospiked surface of the HEA physically damaged the membrane (acting like tiny "pins" puncturing the cell, as evidenced by electron microscopy) and created openings (Figure 6D). Simultaneously, the local electric field at the HEA surface and the ongoing release of Cu^{2+} ions from the alloy worked in concert to generate additional ROS (via catalytic processes) around the bacteria (Figure 6E). The result was a multifaceted attack: The bacteria's membrane was mechanically ruptured and electrically disrupted, and chemically active ions and ROS flooded in to ensure the cell's death (Figure 6B). This synergy of electrostatic attraction, physical membrane penetration, and chemical stress greatly enhanced the bacterial inactivation efficiency of the HEA. Essentially, the HEA acts as both a "magnet" and a "sword" against bacteria, which first attracts them and then delivers a lethal blow. Figure 6F, G investigates the effect of FeNiTiCrMnCu HENPs with different concentrations on the planktonic bacterial count. In 2216E petri dishes, as the copper content in FeNiTiCrMnCu HENPs increases, the number of planktonic cells decreases significantly. Figure 6H, I explores the impact of FeNiTiCrMnCu HENPs at varying concentrations on the viable bacterial count within biofilms. The results indicate that in the presence of HENPs, the percentage of viable bacteria in biofilms decreases significantly. At the same concentration, higher Cu content leads to better antibiofilm performance, indicating that copper content plays a critical role. Through multiple cycling experiments, it demonstrates that the antibacterial ability remains basically stable after 5 cycles of coculturing HENPs with bacteria (Figure 6C). However, a careful observation reveals a slight decrease in antibacterial ability during the third cycle, which may be related to the leaching of copper ions from the nanoparticles.

In summary, high-entropy antibacterial materials can utilize one or more of these mechanisms concurrently. For instance, a Cu-bearing HEA coating might slowly release Cu^{2+} (ion release) while its surface heats under light (a photothermal effect) and its microstructure generates ROS and carries a positive charge for contact killing. Additionally, high-entropy materials exhibit broad-spectrum antibacterial properties. Table 1 summarizes the antibacterial efficacy of selected high-entropy materials against common bacteria. The inherent stability and multifunctionality of HEMs allow these complex mechanisms to operate without significant degradation of the material itself, making them extremely promising for long-term antimicrobial applications.

4. Applications of high-entropy antibacterial materials

Research and development of HEMs have advanced rapidly, but only in recent years have their antibacterial properties attracted broad attention. Due to their combination of potent antimicrobial mechanisms and robust material properties, high-entropy antibacterial materials are being explored in a variety of application domains.

4.1 Biomedical applications

Pathogenic bacteria (and viruses) are a major threat to human health, often causing infections such as gastrointestinal illness (e.g., *E coli*)[107–109] or wound infections (*S aureus*)[110,111], among others. Moreover, the improper use of antibiotics has led to rising antimicrobial resistance, making infections harder to treat. Consequently, the demand for advanced antimicrobial materials in medical applications, including implants, medical devices, wound dressings and healthcare surfaces, has increased because they can prevent or combat infections.

HEAs offer new opportunities in this arena. Many HEAs are highly biocompatible metallic systems (e.g., composed of Ti,

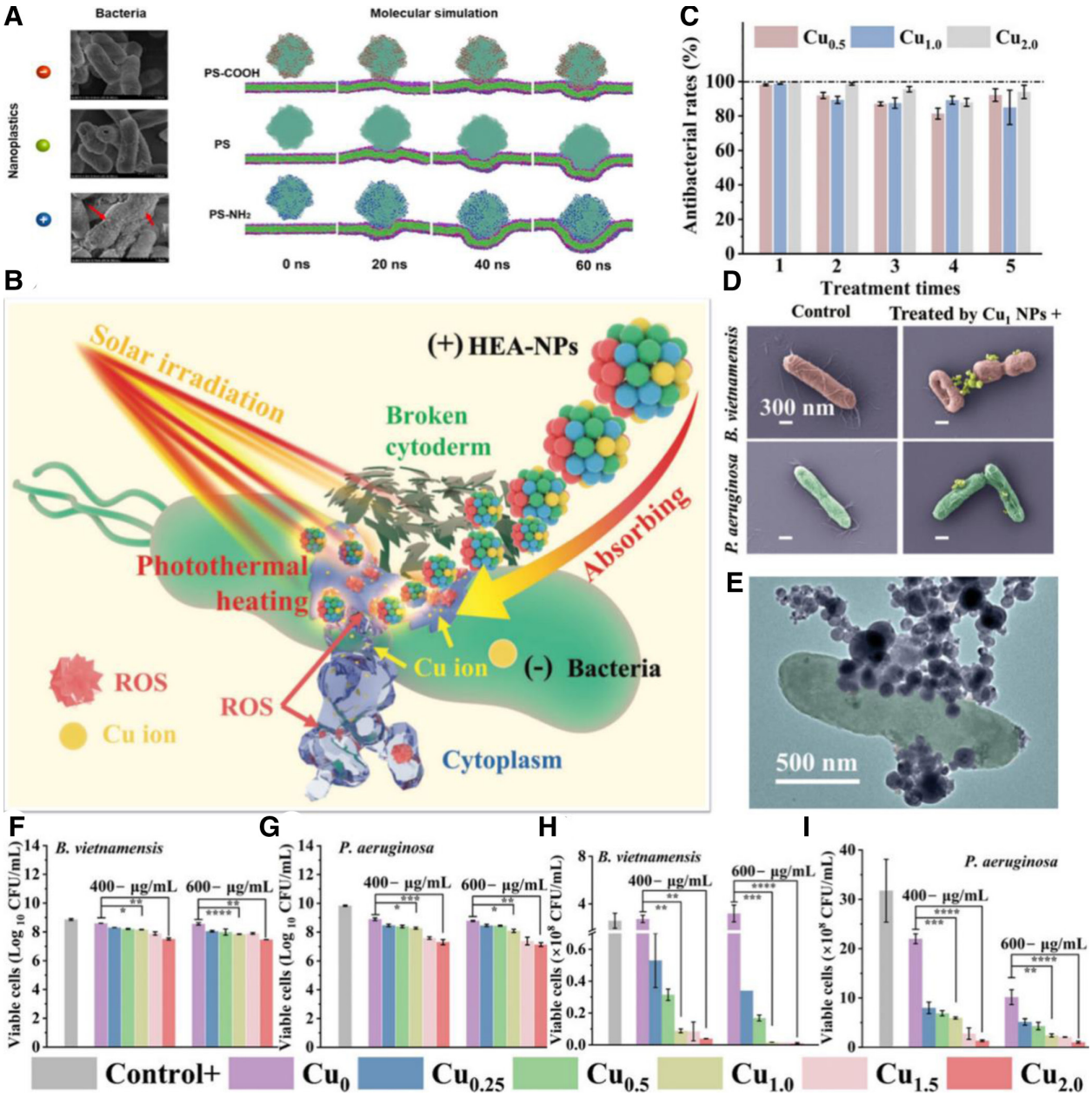

Figure 6. Mechanistic and structural insights into HEA nanoparticle–mediated antimicrobial action. (A) Molecular-dynamics trajectories illustrating the interaction of 16-nm nanoplastics, including negatively charged, neutral, and positively charged, with a model E coli cytoplasmic membrane (POPE: POPG = 3: 1). POPE, 1-palmitoyl-2-oleoyl-sn-glycero-3-phosphoethanolamine; POPG, 1-palmitoyl-2-oleoyl-sn-glycero-3-phosphoryl-glycerol[96]. Copyright 2022 BMC. (B) Schematic of HEA nanoparticle antimicrobial mechanisms combining Cu^{2+} ion release and localized photothermal heating to disrupt bacterial cells and biofilms. (C) Time-cyclic performance by the viable counts of Pseudomonas aeruginosa without light. (D) Scanning electron microscope image showing HEA nanoparticle morphology and surface features. (E) Transmission electron microscope image revealing the internal structure and size distribution of HEA nanoparticles. Antibacterial and antibiofilm properties of HEA-NPs under irradiation. Bacterial cell quantity after incubation with different concentrations of HEA-NPs and then treated with light (1 kW·m^{-2}, 30 min) in 2216E medium: (F) B vietnamensis and (G) P aeruginosa viable planktonic cells, (H) B vietnamensis, and (I) P aeruginosa biofilm sessile cells[97]. Copyright 2023 Wiley-VCH GmbH.

Zr, Ta, and Nb) that have excellent mechanical properties for load-bearing implants. By incorporating antibacterial elements or coatings, HEA-based biomaterials can be made antimicrobial without compromising their structural performance. Ren et al.[102] reported a novel Cu-bearing HEA (with composition $Co_{0.4}Fe$-$Cr_{0.9}Cu_{0.3}$, among other elements) designed for biomedical use (Figure 7E). This HEA demonstrated far superior antibacterial performance compared with standard antibacterial SS. In tests (Figure 7A–D), after 24 hours, the HEA achieved a 99.97% reduction of *E coli* and 99.96% reduction of *S aureus*, essentially complete sterilization. By contrast, a conventional antibacterial SS (containing copper) showed only 71.5% and 80.8% reduction of *E coli* and *S aureus*, respectively. Additionally, the HEA showed higher corrosion resistance than the SS, meaning it is less prone to degradation in physiological environments. Notably, the HEA could be synthesized without excessively complex procedures and maintained excellent mechanical integrity. These results indicate tremendous potential for HEA materials in biomedical applications, such as implant coatings or high-performance antibacterial devices, where they could significantly reduce infection rates.

Another approach is to use HEAs as biocompatible substrates with antimicrobial coatings. Ozdemir et al.[55] developed

Table 1.

Antibacterial activity of HEM-based composites against typical pathogens.

Composition/structure	Synthesis method	Bacterial species	Antibacterial rate	References
$Al_{0.4}CoCrCuFeNi$	Vacuum-induction melting	Pseudomonas aeruginosa Burkholderia vietnamensis	99.99% 99.99%	[79]
$(La_{0.2}Sm_{0.2}Eu_{0.2}Gd_{0.2}Ho_{0.2})_2W_3O_{12}$	High-temperature solid-phasemethod	EV71 H1N1	– –	[101]
$Co_{0.4}FeCr_{0.9}Cu_{0.3}$	Vacuum-arc melting	Staphylococcus aureus	99.96%	[102]
$Al_{0.6}CoCrCu_{0.1}FeNiSi_{0.2}$	Vacuum induction melting	Escherichia coli	100% (3 days)	[103]
$CoCrCu_{0.3}FeNi\text{-}Ag_{(1.8\ wt\%)}$	Vacuum-arc melting	SARS-CoV-2	96% (24 h)	[104]
CoCrCuFeNi	–	Acinetobacter baumannii Methicillin-resistant Staphylococcus aureus	91.74% 99.08%	[105]
$TiVCrMoAlC_3$/CDs	–	Drug-resistant Escherichia coli Bacillus subtilis	99.99% –	[106]

2 biomedical titanium-based HEAs, which are known for their superior mechanical properties and biocompatibility. While these HEAs are strong and corrosion-resistant ideal for implants, they do not inherently kill bacteria. To add antimicrobial functionality, the researchers coated the HEA implants with a thin silver-containing layer designed to release Ag^+ ions. Silver is a potent antimicrobial, but as noted earlier, rapid and uncontrolled release of Ag^+ can be cytotoxic to human cells. They optimized the silver coating process to modulate the Ag^+ release rate (Figure 7F, G). By adjusting coating thickness and deposition parameters, they achieved a balance where the coated HEA released silver ions at a sufficient rate to kill bacteria (showing good antibacterial performance in tests) but not so fast as to harm mammalian cells, thus maintaining cytocompatibility. This work highlights that combining HEAs with controlled-release antimicrobial coatings could produce medical implants that resist infection while remaining safe for human tissue.

Beyond coatings, some HEMs themselves exhibit intrinsic biocompatibility and wound-healing capabilities. He et al.[112] fabricated monolayer high-entropy MXenes that efficiently generated ROS for antibacterial activity, achieving a 67.7% killing rate in vitro. The material also showed excellent photothermal conversion efficiency (65.8% in the NIR-II region)[113,114], and under NIR irradiation, the ROS yield increased significantly, raising the antibacterial efficiency to 96.5%. In vivo studies further revealed accelerated wound-healing in mice, attributed to the synergy of photothermal effects and oxidase-mimicking catalytic activity. Immunofluorescence analysis showed that pro-inflammatory factors such as TNF-α and CD86 were downregulated, indicating a reduction in M1-type macrophages, while anti-inflammatory factors TGF-β and CD206 were upregulated, suggesting polarization toward M2-type macrophages. This M1-to-M2 transition alleviated inflammation and promoted angiogenesis. Collectively, these results highlight that high-entropy MXenes can not only suppress infection but also actively regulate immune responses and vascularization, thereby accelerating tissue repair.

Beyond preventing infections, HEMs are also finding roles in therapeutic interventions. One exciting example involves using HEA nanoparticles for cancer therapy, leveraging their photothermal and catalytic properties to destroy tumor cells (which conceptually overlaps with antibacterial mechanisms). Ai et al.[80] fabricated ultra-small HEA nanoparticles composed of noble metals (PtPdRuRhIr), which exhibited 2 synergistic functions: Strong NIR photothermal conversion (upon 808 nm laser exposure) and intrinsic POD-like activity. These HEA "nanozymes" could thus generate heat and ROS simultaneously (Figure 7H). In a mouse breast cancer model, the HEA nanoparticles (dubbed "HEAzymes") were injected into tumors, and the site was then irradiated with an 808-nm laser twice daily (Figure 7I). The combined photothermal and catalytic action completely eradicated the tumors: By day 7 of treatment, the cancer cells were ablated and the lesions were healing, and by day 14, the tumors had vanished with the wounds fully closed. Thermal imaging confirmed that the HEA nanoparticles rapidly raised the local tumor temperature from 36 to 48 °C under the laser (Figure 7J), contributing to efficient tumor cell killing. While this example is focused on cancer, the underlying mechanisms (photothermal heating and ROS generation by HEA nanoparticles) are the same as those used to kill bacteria. It showcases the versatility of HEA nanomaterials in biomedical therapy. They can be agents for photothermal ablation and disinfection alike. Future antibacterial therapies might employ similar HEA nanoagents to target and destroy bacterial biofilms or localized infections inside the body in a minimally invasive way.

In summary, high-entropy antibacterial materials in the biomedical field can provide: (i) infection-resistant implant surfaces and devices (either via antibacterial alloy composition or antimicrobial coatings on HEA substrates) and (ii) therapeutic nanoparticles that eliminate pathogens or undesired cells via photothermal and catalytic mechanisms. Their high strength, corrosion resistance, and tailorable functionality make them extremely promising for improving healthcare outcomes by preventing implant-related infections and enabling new treatment modalities.

4.2 Public health disinfection

The COVID-19 pandemic has driven home the importance of public sanitation and infection control in communal spaces. There is growing interest in antimicrobial surfaces and coatings for environments such as hospitals, schools, public transit, and shopping centers to reduce the spread of pathogens. HEMs are being explored in this context as durable antimicrobial coatings that can inactivate bacteria and viruses on contact.

Li et al.[45] reported an HEA containing Cu, Fe, Cr, Co, Ni (and a variant with added Al) for use as an antiviral surface coating. As shown in Figure 8A, they prepared a CuFeCrCoNi HEA via vacuum arc melting and assessed its ability to inactivate viruses such as influenza (*H1N1*) and enterovirus 71 (*EV71*), which are responsible for respiratory and

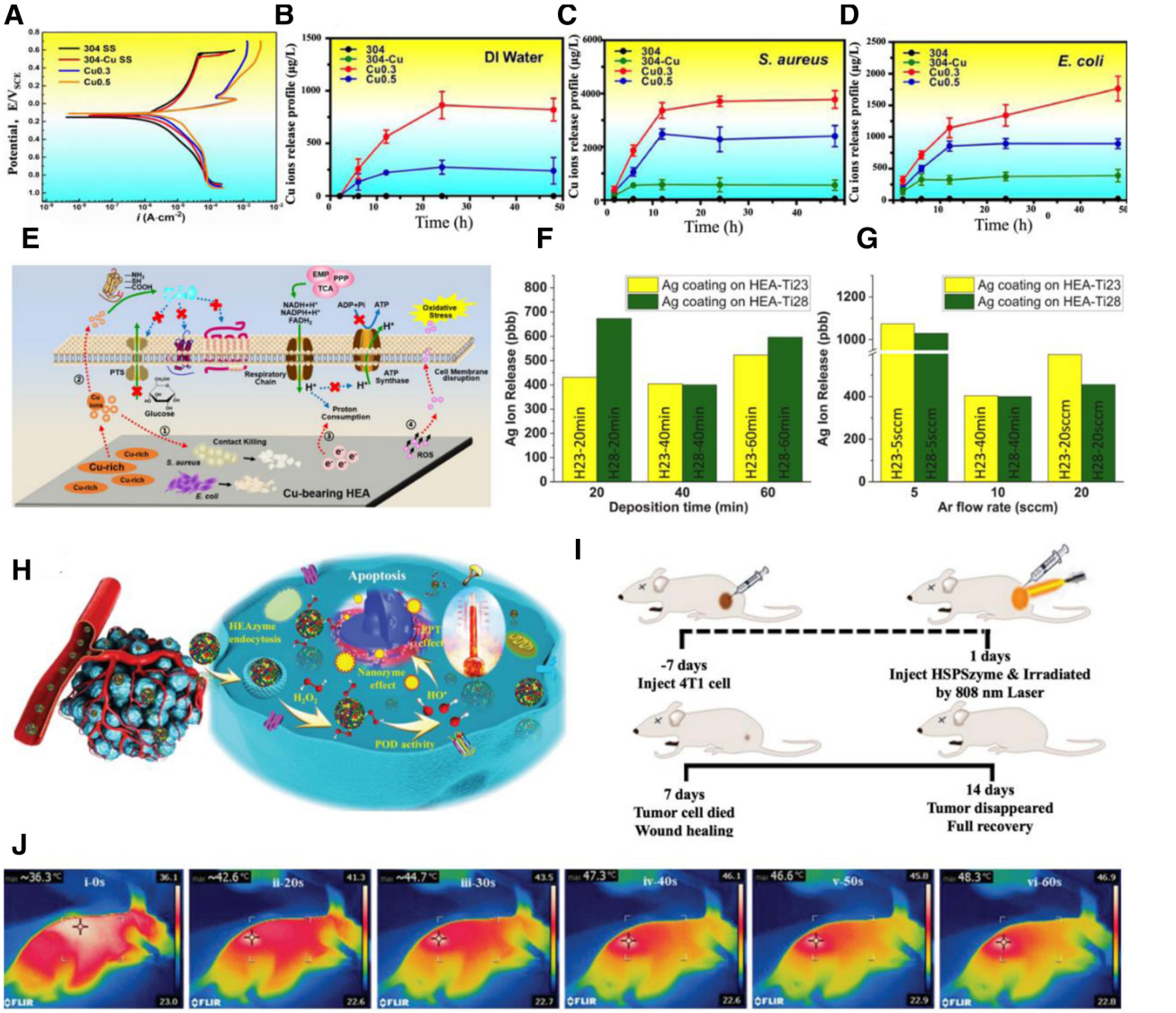

Figure 7. Multifunctional antimicrobial and therapeutic applications of Cu-containing HEAs and HEA nanozymes. (A) Potentiodynamic polarization curves comparing corrosion behavior of 304 SS, Cu-alloyed 304 SS, $Cu_{0.3}$ HEA, and $Cu_{0.5}$ HEA in simulated physiological media. (B–D) Kinetics of Cu^{2+} ion release from $Cu_{0.5}$ HEA coupons into (B) deionized water, (C) E coli suspension, and (D) S aureus suspension over time. (E) The Cu-releasing profile in bacterial suspension of S aureus[102]. Copyright 2022 Elsevier Ltd. (F, G) Ag^{+} release profiles from Ag-doped HEA coatings on HEA-Ti23 and HEA-Ti28 substrates, measured for deposition times of 20, 40, and 60 min at 10 sccm Ar, and for 40 min at varying Ar flow rates (5, 10, and 20 sccm)[55]. Copyright 2023 Elsevier B.V. (H) Illustration of US-HEA nanoparticles as peroxidase-mimetic nanozymes, catalyzing H_2O_2 to generate cytotoxic ·OH for synergistic tumor photothermal therapy. (I) In vivo therapeutic protocol: HEAzyme injection, near-infrared irradiation schedule, and tumor monitoring in a breast cancer mouse model. (J) Infrared thermal images of tumor sites at 0, 20, 30, 40, 50, and 60 s after laser irradiation, demonstrating rapid photothermal heating of HEAzyme-treated tumors[80]. Copyright 2023 Wiley-VCH GmbH.

gastrointestinal infections, respectively (Figure 8D, E). On the HEA surface, both *H1N1* and *EV71* were inactivated by >99.99% within a short exposure time, whereas on a standard 304 SS surface, a large amount of infectious virus remained. This dramatic difference demonstrates that the Cu-containing HEA was highly effective in virus inactivation, likely due to rapid release of Cu^{2+} and perhaps other synergistic effects of the multiple elements (copper and nickel both have known antiviral properties).

To improve the alloy's applicability, a small amount of aluminum was added, creating $Al_{0.4}$CuFeCrCoNi HEA. The addition of Al increased the alloy's corrosion resistance (an important property for long-term use of surfaces) without diminishing its antiviral performance (Figure 8B, C, F, G). The Al-containing HEA also inactivated *H1N1* and *EV71* by ~99.99%. The study noted that appropriate Al alloying improved durability (by forming a protective Al-oxide) but did not negatively affect the release of Cu ions or other antiviral mechanisms. These findings suggest that Cu-bearing HEAs could be deployed as self-disinfecting surfaces in public settings, such as door handles, elevator buttons, or hospital bed rails, where they could continuously kill viruses and bacteria, aiding infection control. Indeed, the authors proposed such HEA coatings for high-touch surfaces in hospitals, schools, and malls to help curb the transmission of viruses such as influenza.

4.3 Industrial wastewater treatment

Environmental sustainability is a pressing global challenge, and wastewater treatment is critical for removing pollutants from industrial and municipal effluents. HEMs are being investigated

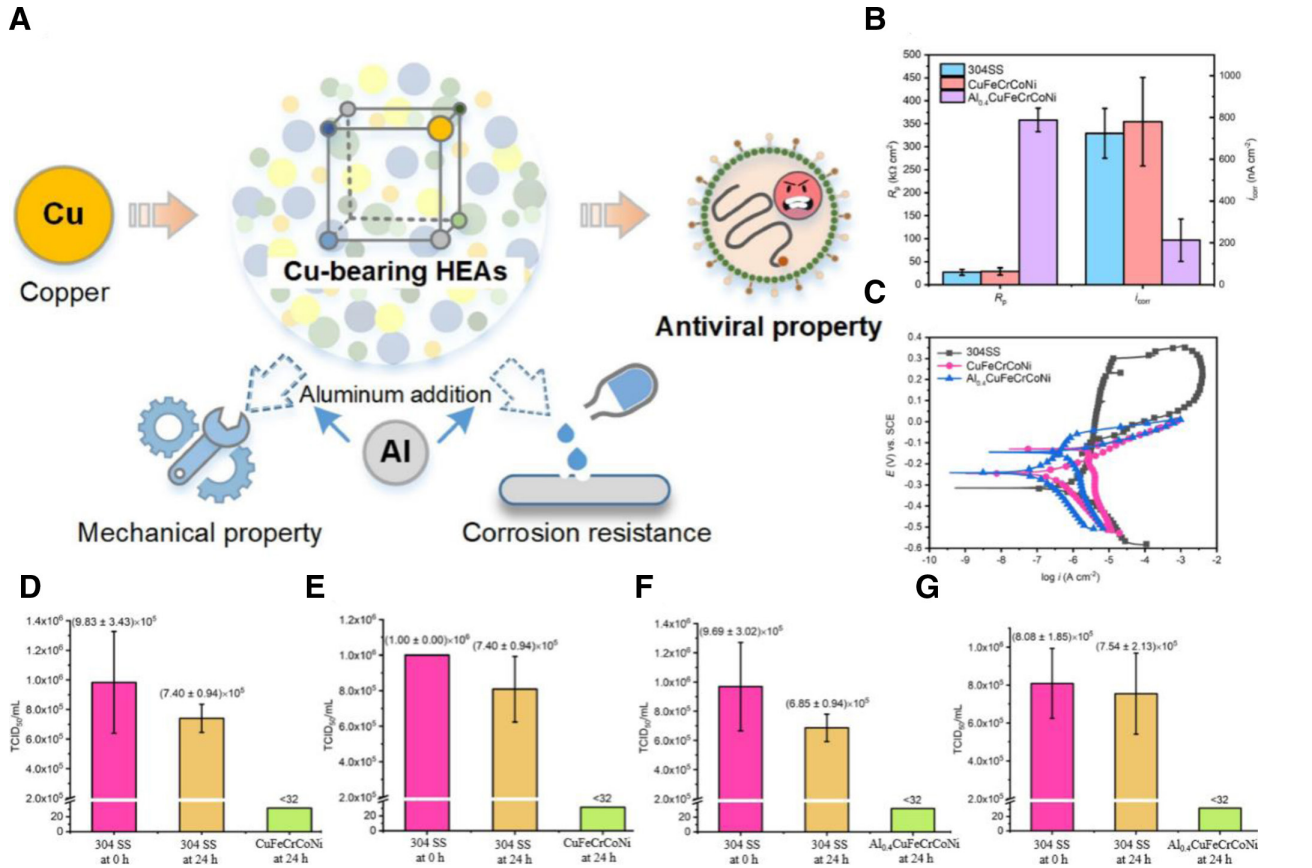

Figure 8. Antiviral and corrosion-resistant properties of HEMs. (A) Schematic illustration of the antibacterial mechanisms and corrosion resistance of Cu-HEAs. (B, C) Electrochemical analysis of the corrosion resistance of 2 Cu-HEAs: (B) Rp and icorr and (C) polarization curves. Standard deviations are from at least 3 parallel tests. Versatile applications of HEA in antiviral and catalytic systems. (D) Inactivation efficiencies of Cu-HEA surfaces against influenza virus H1N1. (E) Inactivation efficiencies of Cu-HEA surfaces against enterovirus 71. Error bars represent standard deviations from at least 3 independent experiments. (F, G) Antiviral properties of the $Al_{0.4}$CuFeCrCoNi HEA against 2 viruses: (F) influenza virus H1N1 and (G) enterovirus 71. Standard deviations are from at least 3 parallel tests[45]. Copyright 2021 Elsevier.

as novel catalysts to degrade organic contaminants and even convert pollutants into less harmful substances through advanced oxidation or reduction processes.

One approach is using HEAs as catalysts in Fenton-like reactions for water purification. Yao et al.[115] immobilized HEA nanoparticles on a nitrogen-doped carbon (NC) support and employed them to activate peroxymonosulfate (PMS) for oxidative degradation of organic pollutants (Figure 9A, B). The HEA served as a catalyst to generate sulfate radicals from PMS, akin to a heterogeneous Fenton catalyst. The resulting HEA-PMS system was tested on real wastewater samples and demonstrated strong tolerance to interference (it maintained activity even in the presence of common inorganic ions and organics). Impressively, it could efficiently remove a suite of 11 different substituted phenol pollutants within 15 minutes (Figure 9C). Moreover, the HEA-PMS system was effective over a broad PH range, indicating versatility for different water conditions (Figure 9D). This suggests that high-entropy catalysts could be used for advanced oxidation processes in wastewater treatment, offering robust performance even in complex water matrices.

Separately, Lv et al.[117] synthesized an AlCoCrTiZn HEA via mechanical alloying and explored its ability to degrade organic dyes. Thanks to the unique atomic-scale structure of the HEA (severe lattice distortion, residual stresses, and high surface area due to nanocrystalline nature), this alloy exhibited a lower activation energy barrier for certain reactions (Figure 9F). In tests, the HEA readily degraded azo dye molecules (a common class of water pollutants from textiles) with high efficiency. HEAs and their oxides, thus, show potential as robust catalysts for breaking down recalcitrant organic compounds in wastewater, an application that benefits from HEAs' chemical stability and tunable active sites.

Another pollutant of concern is nitrate (NO_3^-) in water, which can lead to eutrophication and is problematic in drinking water. Ideally, nitrates could be catalytically reduced to benign products such as nitrogen or selectively converted to useful compounds such as ammonia (NH_3). Liu et al.[116] designed a system using an HEA to catalyze nitrate electroreduction. They prepared a FeNiCoMnRh HEA supported on N-doped carbon, and incorporated it as a cathode catalyst in a Zn-air battery setup to drive nitrate reduction to ammonia. In this decoupled electrolytic system, the HEA/NC served as the cathode (reducing nitrate), while the Zn anode provided electrons (Figure 9E). The HEA catalyst exhibited a specific response to nitrate: significant cathodic current was observed around –0.3 V (versus Hg/HgO reference) only when nitrate was present, and almost no current in its absence (Figure 9G). This indicated that the HEA was highly selective and active for nitrate reduction. Using this HEA-based system, nitrate was converted to ammonia with high efficiency, offering a novel route for energy-efficient wastewater treatment that simultaneously produces ammonia (a valuable chemical). The use of a high-entropy catalyst was key

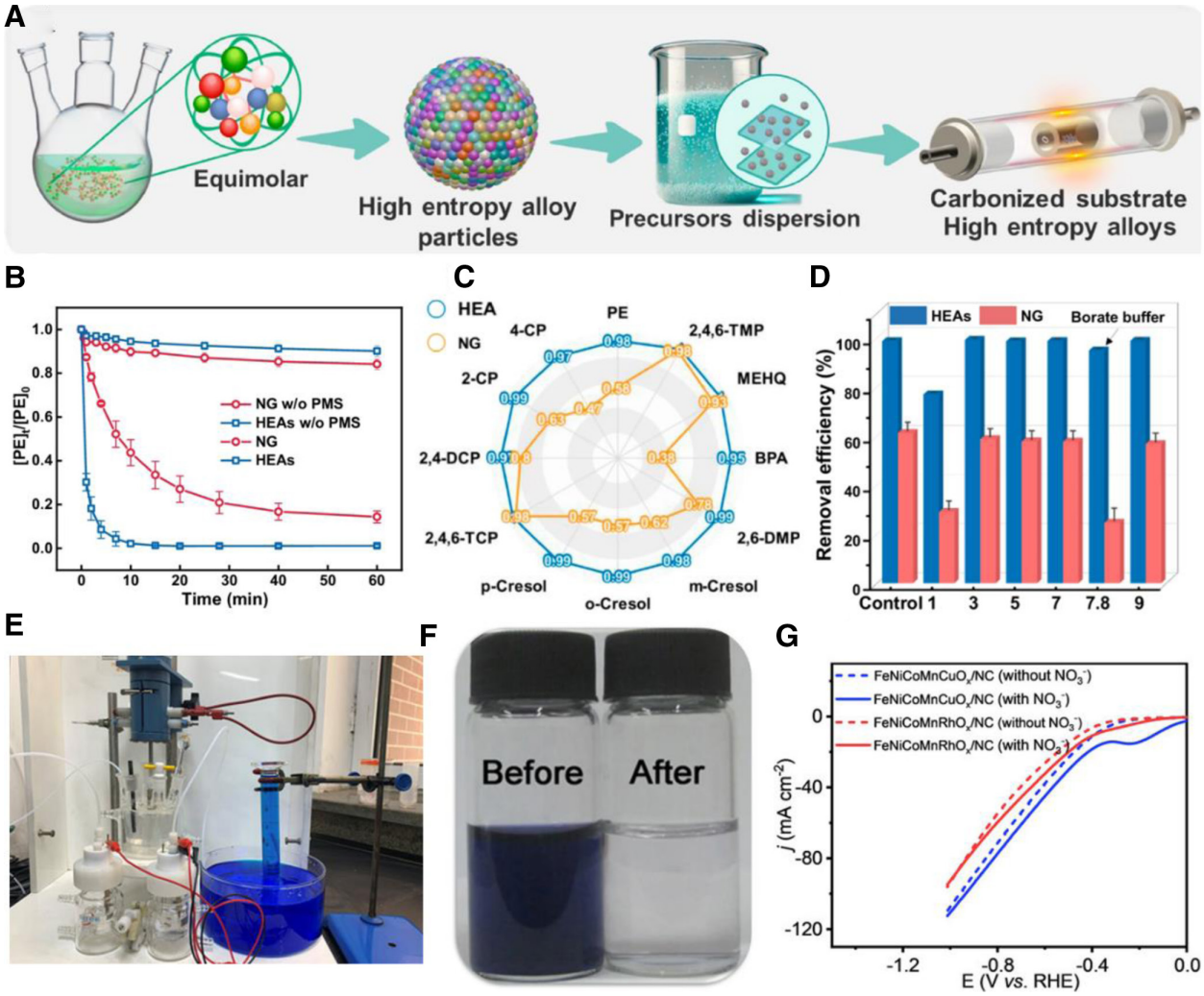

Figure 9. HEAs for wastewater treatment and organic dye degradation. (A) The schematic diagram for the synthesis process of HEAs. (B) HEAs and N-doped graphene catalytic removal efficiency of phenol with interference of 5/10 mM salts and humic acid. (C) Evaluate the removal efficiency of different pollutants in the High-entropy alloys-peroxymonosulfate system and the N-doped graphene-peroxymonosulfate system within 15 min. (D) HEAs and N-doped graphene catalytic removal efficiency of phenol under different pH and borate buffer environments[115]. Copyright 2025 Spring Nature. (E) The top view of the structural configuration of PMS on HEAs[116]. Copyright 2025 Wiley-VCH GmbH. (F) Appearances of the DB6 solution before and after degradation by S1[117]. Copyright 2016 Spring Nature. (G) Linear scanning voltammetry curves in 0.5 M NaOH with 0.25 M NO_3^--N electrolyte[116]. Copyright 2025 Wiley-VCH GmbH.

to this performance, as the multiple elements provided a range of active sites and a "cocktail effect" that enhanced electron utilization and reaction kinetics.

In summary, HEMs in wastewater treatment can function as catalysts for pollutant degradation or conversion. Their structural disorder and multicomponent surfaces can be advantageous in activating oxidants (such as PMS) to generate radicals for oxidation of organics, or in facilitating multielectron reduction processes (such as nitrate-to-ammonia). Furthermore, their typically high corrosion resistance ensures durability in harsh aqueous environments. These features make HEAs and high-entropy oxides very attractive for developing next-generation water treatment technologies aimed at sustainable pollution mitigation.

4.4 Marine and shipbuilding applications

Marine environments are extremely challenging for materials due to constant exposure to saltwater, biofouling organisms, and mechanical wear from waves and tides. Ships and marine structures suffer from corrosion and biofilm growth, which can lead to structural damage and increased drag (fuel inefficiency). HEAs, with their outstanding corrosion and wear resistance, are being explored as new materials for marine applications, including as antibacterial, antifouling coatings to protect ship hulls and components.

Ships are typically made of various metals, creating galvanic potential differences. In seawater (an electrolyte), galvanic corrosion cells can form between different metals, accelerating overall corrosion[118–120]. Additionally, ships that carry organic cargo or fuel may have tanks where organic compounds exacerbate corrosion. Mechanical forces such as waves, tides, and suspended particles also cause continuous erosion and abrasion of surfaces, damaging protective coatings and exposing fresh metal to corrosive attack[121,122]. Combining these factors, marine corrosion is severe and leads to frequent maintenance and repairs. HEAs are promising as corrosion-resistant coatings or components in such conditions[123]. Many HEAs form protective passive films (rich in Cr, Al, etc), and their sluggish diffusion and cocktail effects can impart superior resistance to uniform and localized corrosion. They also tend to have high hardness and thus good erosion resistance.

One issue encountered in some HEAs is the tendency for certain elements (such as copper) to segregate, which can induce galvanic microcouples and reduce corrosion resistance or cause embrittlement. Verma et al.[125] found that in as-cast CoCrFeNiCu$_x$ HEAs, increasing Cu content reduced the wear rate (improving wear resistance), but large-scale segregation of Cu could deteriorate corrosion behavior and even cause brittleness. The key is to refine the microstructure so that copper (or other additives) is uniformly distributed. Liu et al.[126] addressed this by adjusting the processing of a Cu-containing HEA to achieve a nanoscale homogeneous distribution of Cu, thereby retaining the HEA's excellent bulk properties while minimizing galvanic microcells. The optimized HEA showed minimal adverse effect from Cu addition and even improved antifouling and friction performance (likely by leveraging Cu's biocidal effect without sacrificing alloy integrity).

To protect against marine biofouling and corrosion, high-entropy coatings are being investigated. Wang et al.[127] deposited a refractory high-entropy carbide coating, (TiZrNbTaMo)C, on a Ti alloy substrate to test its tribocorrosion performance in artificial seawater. The HEA carbide coating exhibited a much lower corrosion potential and current density compared with the bare Ti alloy, indicating significantly better corrosion resistance (it acted as a noble, protective layer). The coating also resisted chloride ion penetration/adsorption better than the uncoated alloy. Importantly, under sliding wear in saltwater, the HEA coating showed excellent tribocorrosion behavior, maintaining integrity without pitting. This suggests such HEA coatings could protect mechanical parts (such as propellers, pumps, and valves) in marine systems by simultaneously reducing wear and corrosion.

Another crucial consideration is microbiologically influenced corrosion (MIC) and biofouling by marine organisms (e.g., algae, bacteria, and barnacles). Han et al.[124] applied a laser-cladded FeCrNiCuAl$_x$ HEA coating onto 304 SS and studied how varying aluminum content (x) affected its corrosion and antibacterial performance (Figure 10C). At an optimal Al content (approximately 1.2 in atomic ratio), the HEA coating formed a unique nanostructured, interwoven microstructure with nanoscale precipitates. This Al$_{1.2}$ HEA coating exhibited the best corrosion resistance among the tested compositions and also demonstrated strong antibacterial effects against *P aeruginosa*, a common marine bacterium that contributes to biofilm formation and MIC. After 24 h of exposure to *P aeruginosa*, live/dead staining showed that the HEA-coated surface had far fewer viable bacteria than the uncoated steel (the 304 SS control had a thick biofilm with many live cells, whereas the HEA coating had only a sparse presence of bacteria), as shown in Figure 10A. Surface profilometry and confocal microscopy revealed that the 304 SS developed deep corrosion pits (~6.14 μm deep) under the biofilm, while the HEA coating showed only minor surface corrosion products and much shallower attack. The biofilm thickness on the HEA coating was only ~15 μm, compared with ~63 μm on 304 SS, indicating a 4-fold reduction (Figure 10B). This indicates that the HEA coating not only resisted bacterial corrosion but also significantly inhibited biofilm growth (Al$_{1.2}$ seemed to provide the best antiadhesion property). The authors concluded that the Al-containing HEA coating could effectively mitigate marine biofouling and MIC, and that its excellent performance provides a new strategy for ship coating design. By reducing biofilm formation, such coatings can decrease drag on ship hulls and protect against corrosion, enhancing both efficiency and longevity of marine vessels.

In addition, nicotinamide mononucleotide (NMN) can be rapidly absorbed in vivo and converted into nicotinamide adenine dinucleotide[128], the increase of which inhibits ROS-induced pyroptosis and reduces the production of pro-inflammatory cytokines. Based on this concept, Zhang et al.[129] developed an ultrathin high-entropy hydrotalcite (CeZnMnMgAl-based) with abundant oxygen vacancies, highly dispersed multimetallic sites, and significant lattice distortion. These structural features endowed the hydrotalcite with an appropriate bandgap and excellent singlet oxygen generation activity under ultrasound irradiation. Subsequently, the ultrathin high-entropy hydrotalcite was incorporated into a thermoresponsive Pluronic F127 hydrogel loaded with NMN[130]. Under ultrasound irradiation, this composite could rapidly produce singlet oxygen and effectively kill multidrug-resistant bacteria. Moreover, when the ultrasound was stopped, the redox enzyme-mimicking catalytic activity of the high-entropy hydrotalcite and the sustained release of NMN significantly alleviated inflammation. In in vivo experiments using a mouse model infected with methicillin-resistant *Staphylococcus aureus* (MRSA), the material notably promoted tissue recovery and wound-healing, with no obvious toxic side effects or weight loss. In vitro experiments further demonstrated that under ultrasound, the material could effectively disrupt MRSA and *E coli* membranes and biofilms, while also exhibiting good biocompatibility and anti-inflammatory capability.

Building on this, Yang et al.[131] developed Al$_x$CoCrCuFeNi HEAs with varying Al contents. The addition of Al increased the polarization resistance by nearly twentyfold compared with the Al-free alloy, markedly enhancing corrosion resistance. Moreover, the alloy suppressed microbial adhesion and growth through a dual mechanism of Cu^{2+} ion release and ROS generation, thereby improving antifouling capability. In a complementary approach, Yu et al.[132] designed a high-entropy oxide nanozyme coating, which exhibited multienzyme-mimicking activities and strong photothermal conversion due to the synergistic action of multiple cations and defect engineering. When blended with polyurethane, the coating drastically reduced bacterial survival and inhibited biofilm formation, underscoring its potential for marine antifouling. Process optimization can further improve performance. Wang et al.[133] employed high-velocity oxygen fuel spraying to deposit a dense FeCrNiCoAl HEA coating onto steel substrates. In artificial seawater tests, the HEA coating exhibited a corrosion rate only one-fifth that of 304 SS or conventionally cast HEAs, demonstrating outstanding long-term corrosion resistance.

In summary, HEMs hold great promise in marine and shipbuilding applications by offering integrated antifouling and anticorrosion capabilities. They can serve as advanced coating materials that withstand the harsh marine environment better than traditional single-metal coatings. Their broad-spectrum antibacterial properties (e.g., due to Cu and Ag) help prevent biofilm and barnacle attachment, while their high corrosion resistance and hardness protect against chemical and mechanical degradation. These features could reduce maintenance costs and extend the service life of ships and offshore structures. As research progresses, we may see HEA coatings becoming a new standard for maritime anticorrosion technology.

Here, we review 4 key areas where these materials show significant promise: (1) biomedical applications, (2) public health disinfection, (3) industrial wastewater treatment, and (4) marine (shipbuilding) applications, as summarized in Table 2.

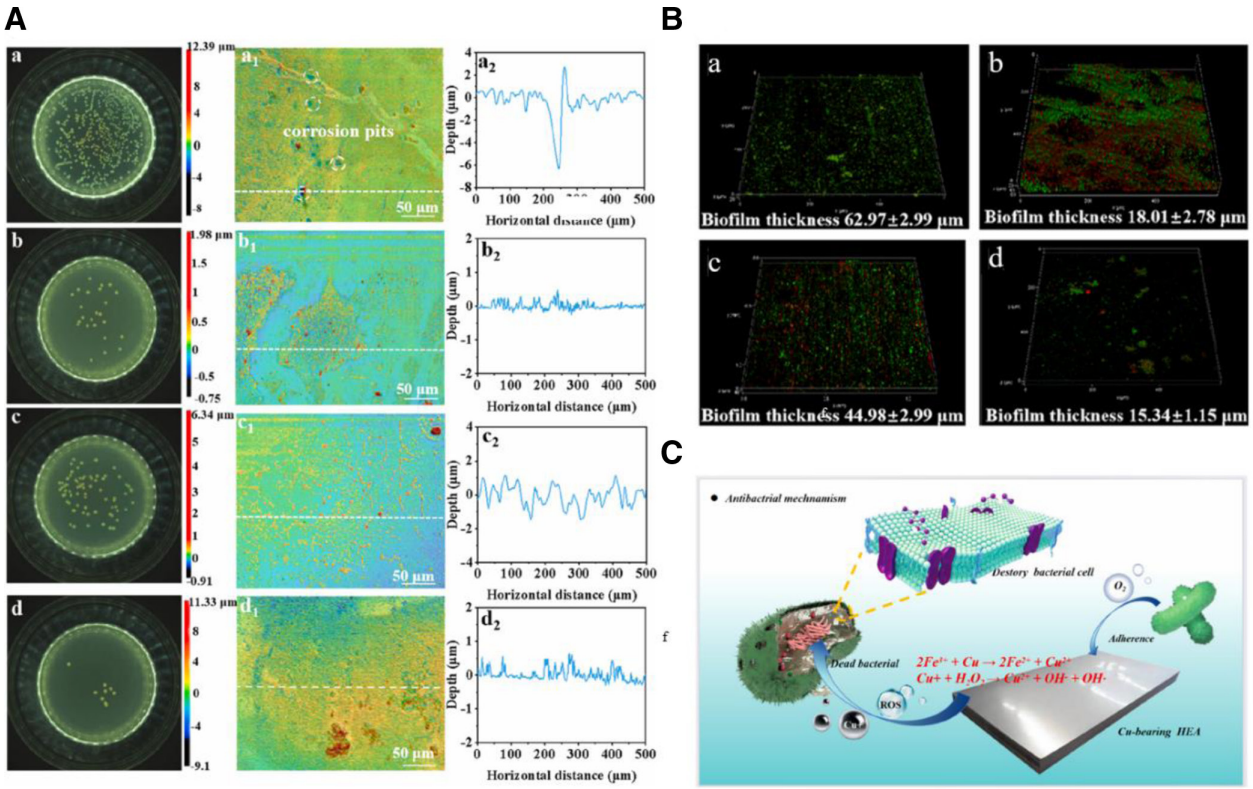

Figure 10. Antibacterial performance and anticorrosion characteristics of Al-doped HEA coatings. (A) Confocal laser scanning microscope images of live/dead stained Pseudomonas aeruginosa biofilms on (a) 304 SS, (b) Al_0 HEA, (c) $Al_{0.8}$HEA, and (d) $Al_{1.2}$HEA surfaces after 24 h incubation. Panels (a1–d1) show live (green) and dead (red) cell staining; panels (a2–d2) present corresponding 3D surface topography maps. (B) Quantitative analysis of corrosion pit depths for (a) 304 SS, (b) Al_0HEA, (c) $Al_{0.8}$HEA, and (d) $Al_{1.2}$ HEA after microbial exposure. (C) Schematic illustrating the antibacterial mechanism of HEA coatings[124]. Copyright 2025 Elsevier.

5.Challenges and outlook

Despite the promising advances in high-entropy antibacterial materials, several challenges must be addressed before these materials can achieve widespread practical adoption. In this section, we outline the key challenges and then discuss the outlook and future directions, including the importance of interdisciplinary research and process innovation.

5.1 Current challenges

- Complex composition design: The very feature that gives HEMs their unique properties, such as a multitude of elements in a single material, also makes rational design extremely challenging. With so many components and possible combinations, predicting the phase formation and properties of HEAs is difficult[138,139]. When designing an HEMs for antibacterial performance, one must consider not only the antimicrobial efficacy but also how the addition of certain elements (and their concentrations) will affect phase stability, mechanical properties, corrosion behavior, etc. For example, adding a bioactive element such as Cu or Ag in different amounts can drastically change the alloy's microstructure and entropy, thereby influencing not just bacterial killing ability but also strength and ductility. The compositional design space is enormous, and optimizing a material for multiple performance criteria requires complex trade-offs and extensive experimentation or computational guidance. Screening through endless combinations to find an "optimal" formulation is time-consuming and often inefficient. This complexity means that achieving the best overall performance (antibacterial efficacy and other properties) is very challenging and currently often done by trial-and-error. Design strategies and tools (such as high-throughput computation or machine learning) are still needed to navigate this vast compositional landscape more efficiently.
- Biosafety and environmental impact: High-entropy antibacterial materials typically contain multiple heavy metals or oxides. If these materials are to be used in biomedical implants or in environmental settings (such as water treatment or marine coatings), it is crucial to ensure they do not pose long-term toxicity or ecological risks. Preliminary studies suggest that certain HEAs (e.g., TiZrHfNbTa-based alloys) are cytocompatible in the short term, but the long-term effects of HEMs in the human body or environment remain unclear. Do the corrosion or wear products of an HEA (which may contain Ni, Co, etc) cause any chronic toxicity? If nanoparticles of HEA are introduced into the body (for therapy) or released into waterways (from coatings), what happens to them over time? These questions require thorough investigation. Large-scale application will demand detailed biosafety evaluations to ensure that HEMs (or their degradation products) do not harm human health or accumulate in ecosystems. In particular, if an HEA releases metal ions as part of its antibacterial action, one must ensure the concentration stays below harmful thresholds for humans and nontarget organisms. Developing strategies to mitigate any potential toxicity—for instance, by adding elements to neutralize harmful ions or by

Table 2.

Recent advances in high-entropy antibacterial materials.

Composition/structure	Synthesis method	Application	Performance summary	References
FeMnCoTiVCu	Mechanical alloying	Wastewater treatment	Exhibits >99% antibacterial rates against E coli and S aureus even without light activation.	[65]
$Al_{0.4}$ CoCrCuFeNi	High-temperature solid-state reaction	-	Achieves nearly 100% killing of Pseudomonas aeruginosa and 99.99% of Bacillus velezensis.	[79]
PtPdRuRhIr	Metal–ligand crosslinking	Photothermal cancer therapy	Nanoparticles exhibit concentration-dependent cytotoxicity to cancer cells with minimal toxicity to normal cells; effective photothermal ablation under 808 nm NIR laser.	[80]
FeNiTiCrMnCux	Nonequilibrium arc discharge plasma	Marine biofouling/ corrosion	Under illumination, photothermal effect enhances antibiofilm, antibacterial efficacy: $Cu_{0.1}$-HEA-NPs increase antibiofilm rate from 81% to 97.4% for P aeruginosa.	[97]
$(La_{0.2}Sm_{0.2}Eu_{0.2}Gd_{0.2}Ho_{0.2})_2W_3O_{12}$	High-temperature solid-state reaction	-	Antibacterial efficiency >99.9% against S aureus and E coli.	[101]
$Co_{0.4}FeCr_{0.9}Cux$	Vacuum arc melting	-	At x = 0.3, achieves 99.97% (E coli) and 99.96% (S aureus) killing after 24 h, far surpassing traditional antibacterial SS.	[102]
$CoCrCu_{0.3}FeNi$ -Ag(1.8 wt%)	Vacuum induction melting	-	Exhibits >99.9% antibacterial efficacy against Pseudomonas aeruginosa (Gram–) and Bacillus velezensis (Gram+).	[104]
$Cu_{12}Pd_{11}Fe_{10}Co_{11}Ni_{12}$	Vacuum arc remelting	Organic wastewater treatment	HEA-PMS system degrades phenol with over 7-fold higher efficiency than N-doped graphene; exhibits rapid kinetics for various phenolic pollutants, strong anti-interference, and stability over a wide pH range.	[115]
AlxCoCrCuFeN	Vacuum arc melting	Marine alloys	Against Pseudomonas aeruginosa, $Al_{0.1}$-HEA achieves 99.99% antibiofilm efficiency; after 7 days, efficiency remains 99.87%.	[131]
ZrNbTiCrCu	Magnetron sputtering	Biomedical	At a sputtering current of 0.6 A, demonstrates excellent biocompatibility (>95% cell viability) and 96.2% antibacterial rate.	[134]
TiZrNbTaxGa	Arc melting	Bone implant material	In vivo experiments show that 1% Ga-doped alloy inhibits biofilm infection, alleviates inflammation, and reduces bacterial load.	[135]
$(TiZr)_{80}(NbTa)_{20}$-xCux	Arc melting	Biomedical implant alloy	At x = 7.5 at%, antibacterial rate against E coli and S aureus exceeds 90% with good biocompatibility.	[136]
$Ti_{50}Zr_{25}Nb_{20}$ Cu_5-xAgx	Biomedical implant alloy	Biomedical implant alloy	At x = 2.5, shows 99% antibacterial efficiency against S aureus; inhibits biofilm formation.	[137]

applying safe coatings over HEA implants that only activate when needed—will be important. Likewise, studying the environmental fate of HEA nanoparticles or dissolved species will be necessary for regulatory approvals.

- HEMs often incorporate multiple heavy metals or oxides. For their safe use in biomedical implants, water treatment systems, or marine coatings, it is critical to ensure that they do not pose long-term toxicity or ecological risks. Preliminary studies suggest that certain HEAs (e.g., TiZrHfNbTa alloys) show short-term cytocompatibility, but long-term effects in vivo or in ecosystems remain unclear. Do corrosion or wear products of HEAs containing Ni, Co, or similar elements cause chronic toxicity? If HEM nanoparticles are used in biomedical therapies or released into waterways from coatings, how do they behave over time? Answering these questions will require systematic biosafety and ecotoxicological evaluations. Moreover, since many antibacterial HEMs rely on controlled ion release, it is essential to ensure that the released ion concentrations remain below harmful thresholds for humans and nontarget organisms. Several strategies may mitigate such risks. For example, microstructural control can regulate ion release: Ozdemir et al. demonstrated that optimizing the deposition conditions of Ag coatings on Ti-based HEAs allowed precise control over Ag^+ release, thereby minimizing environmental hazards. Similarly, enhancing passive film formation can protect the substrate: Medina et al.[140] showed that tuning the Ta or W content expanded the passivation range of CrFeNi-based HEAs, producing stable protective oxide films. In addition, advanced processing techniques can improve coating density and stability: Jia et al.[141] employed laser melting deposition to fabricate defect-free CoCrNbNiW HEA coatings with enhanced hardness and wear resistance, indirectly reducing surface degradation and ion leaching. These examples suggest that careful compositional tuning and processing innovation can significantly lower the risks of elemental leaching and improve environmental compatibility, but systematic long-term studies remain lacking.

5.2 Future perspectives

Addressing the above challenges and advancing high-entropy antibacterial materials will likely require a combination of multidisciplinary research efforts and innovations in fabrication techniques. Below, we outline some key perspectives:

- Multidisciplinary research and material innovation: The development of high-entropy antimicrobial materials will benefit from the deep integration of materials science with physics, chemistry, biology, and medicine. By combining insights from these disciplines, researchers can achieve a

more comprehensive understanding of how composition and structure relate to performance. For instance, using surface physics and electrochemistry, one can probe the detailed interactions between an HEA surface and bacterial membranes (e.g., how the work function or surface charge of the alloy influences bacterial adhesion). Theoretical modeling and simulations (quantum calculations, molecular dynamics, etc.) can help screen compositions and predict stable phases or likely properties, significantly speeding up the discovery of new HEAs with desired antibacterial traits. Meanwhile, collaboration with microbiologists and medical scientists is essential to study the interactions of HEAs with cells and to establish rigorous biosafety evaluation systems. Future research might involve in situ imaging techniques (such as advanced microscopy) to watch how HEA particles degrade in the body or how bacteria respond at the molecular level when contacting an HEA surface. At present, most research on high-entropy antibacterial materials remains at the preclinical stage, with the majority of studies focusing on in vitro experiments and small-animal models, while systematic clinical studies are still limited. The use of advanced characterization and monitoring technologies will be crucial to promote clinical translation. For example, Real-time biomedical imaging could, for example, track the degradation of an HEA implant in vivo and the distribution of released metal ions, informing how to optimize the material's design. Overall, an interdisciplinary approach will accelerate innovation-leading to HEMs that are not only effective against microbes but also safe and reliable for clinical or environmental use.

- Process innovation and industrialization: Developing cost-effective, scalable fabrication methods will determine whether high-entropy antibacterial materials can transition from the lab to real-world applications. On one hand, traditional processes such as casting, thermal spraying, and powder sintering can be optimized. For example, improving thermal spray parameters can produce denser HEA coatings with fewer pores, thereby enhancing their protective quality. On the other hand, entirely new processes may emerge. The advent of additive manufacturing (3D printing) offers a powerful tool for fabricating complex HEA components with customized shapes and compositions. Already, researchers have combined HEA development with 3D printing to create architectured materials[142–145]. In the context of antimicrobial materials, 3D printing could enable patient-specific HEA implants or tailored porous structures that fit unique anatomical needs while providing antibacterial function. For industrial scaling, processes such as rapid solidification, mechanochemical synthesis, or even in situ alloying during part fabrication (as in some directed energy deposition methods) could lower costs and allow mass production. Another promising direction is thin-film deposition techniques (such as magnetron sputtering or pulsed laser deposition) to create high-entropy coatings on large surfaces uniformly—this is crucial for covering hospital surfaces or ship hulls. As these fabrication technologies mature and become more economical, we can expect high-entropy antibacterial materials to find broader use in healthcare, food processing, water treatment, marine transportation, and more[146]. Industrial uptake will also be spurred by demonstrating clear technical advantages (e.g., significantly longer service life and reduced infection rates) that justify the switch to these new materials.

In conclusion, high-entropy antibacterial materials represent a cutting-edge solution to longstanding challenges posed by microbial infections. They uniquely combine the broad-spectrum antimicrobial efficacy (through multipronged mechanisms such as ion release, photothermal effect, ROS generation, and electrostatic disruption) with the structural and chemical robustness inherent to high-entropy compositions. This dual advantage means they can combat microbes while also serving as durable engineering materials. Although there are hurdles to overcome—chiefly in optimizing complex compositions and verifying long-term safety—the field is rapidly progressing. With continued multidisciplinary research, clever design strategies, and advances in manufacturing, high-entropy antimicrobial materials are poised to become important tools for safeguarding human health and improving industrial processes. They offer an innovative pathway toward solving global bacterial infection problems, whether it be reducing hospital-acquired infections, keeping public spaces sanitary, treating polluted water, or protecting ships at sea. The ongoing developments reviewed here pave the way for these HEMs to transition from experimental prototypes to impactful real-world applications in the near future.

Acknowledgements

This work was financially supported by the Joint Fund Project of the Major Science and Technology Projects of Gansu Province (Grant No. 25ZDGF001), the CAS "Light of West China" Program, and Shihezi University-Level Independent Funding Support Program (Grant No. ZZZC2023038).

Conflict of interest

The authors declare that they have no conflicts of interest.

References

[1] Chang J, Xiong J, Jia H, et al. Polyiodo azole-based metal–organic framework energetic biocidal material for synergetic sterilization applications. *ACS Appl Mater Interfaces*. 2023;15(39):45668–45675.
[2] Yang J, Liu K, Chen Y, et al. A supramolecular bactericidal material for preventing and treating plant-associated biofilms. *Nat Commun*. 2025;16(1):2627.
[3] Reyna VF. Decision-making about risk in the era of the novel coronavirus disease. *Chest*. 2020;158(4):1310–1311.
[4] Crowley S, Cassidy E. Comparing psychiatric admission following suicidal presentations to the emergency department pre-COVID and during the COVID era. *Eur Psychiatry*. 2024;67(S1):S263–S264.
[5] McKercher B, Tkaczynski A. The reticent tourist in a COVID-adapted world. *Tour Manag*. 2024;103:104885.
[6] Mueller MR, Ganesh R, Hurt RT, et al. Post-covid conditions. *Mayo Clin Proc*. 2023;98(7):1071–1078.
[7] van Elsland D, Neefjes J. Bacterial infections and cancer. *EMBO Rep*. 2018;19(11):e46632.
[8] Aung NM, Nyein PP, Kyi MM, et al. Bacterial coinfection in adults with severe malaria. *Clin Infect Dis*. 2020;72(3):535–536.
[9] Chaukimath P, Frankel G, Visweswariah SS. The metabolic impact of bacterial infection in the gut. *FEBS J*. 2022;290(16):3928–3945.
[10] Wernicki A, Nowaczek A, Urban-Chmiel R. Bacteriophage therapy to combat bacterial infections in poultry. *Virol J*. 2017;14(1):179.
[11] Jiang J, Ding X, Isaacson KP, et al. Ethanol-based disinfectant sprays drive rapid changes in the chemical composition of indoor air in residential buildings. *J Hazard Mater Lett*. 2021;2:100042.
[12] Boyce JM. Alcohols as surface disinfectants in healthcare settings. *Infect Control Hosp Epidemiol*. 2018;39(3):323–328.
[13] Wang B, Yi H, Xu K, et al. Prediction of the self-accelerating decomposition temperature of organic peroxides using qspr models. *J Therm Anal Calorim*. 2016;128(1):399–406.

[14] Duan L, Yun Q, Jiang G, et al. A review of chloride ions removal from high chloride industrial wastewater: sources, hazards, and mechanisms. *J Environ Manage*. 2024;353:120184.
[15] Wu D, Hu Y, Liu Y, et al. Review of chloride ion detection technology in water. *Appl Sci*. 2021;11(23):11137.
[16] Wu Z, David SA, Feng Z, et al. Weldability of a high entropy CrMnFeCoNi alloy. *Scr Mater*. 2016;124:81–85.
[17] Paul TR, Belova IV, Murch GE. Analysis of diffusion in high entropy alloys. *Mater Chem Phys*. 2018;210:301–308.
[18] Asadikiya M, Yang S, Zhang Y, et al. A review of the design of high-entropy aluminum alloys: a pathway for novel al alloys. *J Mater Sci*. 2021;56(21):12093–12110.
[19] Wang Z, Xing F, Xu G, et al. Microstructure and mechanical properties of additive manufactured tic-reinforced $Fe_{55}Cr_{25}Co_{10}Ni_{10}$ high-entropy alloy composites. *Opt Laser Technol*. 2025;187:112870.
[20] Osman H, Liu L, Pan J, et al. Effect of tic addition on the microstructure and mechanical properties of FeCoCrNiMn high entropy alloy fabricated by selective laser melting. *J Alloys Compd*. 2024;982:173583.
[21] Gómez-Esparza CD, Rodríguez-Gónzalez CA, Estrada-Guel I, et al. An analysis of nanoindentation in a NiCoAlFeMo high entropy alloy produced by sintering. *Microsc Microanal*. 2017;23(S1):772–773.
[22] Lei Y, Liu H, Zhang F, et al. Electrochemical corrosion behavior of spinel-like high-entropy oxide $(CrMnFeCoNi)_3O_4$ and $(CrMnFeCoZr)_3O_4$/epoxy coatings. *Mater Lett*. 2024;370:136816.
[23] Xiao X, Lin M, Xu C, et al. An efficient approach to develop and screen out high-entropy alloy composition with high performance for biomedical application. *Surf Coat Technol*. 2024;478:130504.
[24] Zhang L, Chen L, Wang J, et al. High entropy engineering boosts thermo-mechanical properties of rare-earth tantalates: influences of cocktail effects. *J Materiomics*. 2025;11(4):100984.
[25] Hsu W-L, Tsai C-W, Yeh A-C, et al. Clarifying the four core effects of high-entropy materials. *Nat Rev Chem*. 2024;8(6):471–485.
[26] Zhang S, Wang T, Zhang G, et al. Current status of research on the application of high-entropy alloys in the field of brazing. *Weld World*. 2025;69(6):1705–1720.
[27] He C-Y, Li Y, Zhou Z-H, et al. High-entropy photothermal materials. *Adv Mater*. 2024;36(24):2400920.
[28] Hamedani SAN, Amjad-Iranagh S, Dehghani K. Photothermal high-entropy materials: a review. *Sustain Mater Technol*. 2025;43:e01316.
[29] Yeh J-W, Chen S-K, Lin S-J, et al. Nanostructured high-entropy alloys with multiple principal elements: novel alloy design concepts and outcomes. *Adv Eng Mater*. 2004;6(5):299–303.
[30] Cheng C-Y, Yang Y-C, Zhong Y-Z, et al. Physical metallurgy of concentrated solid solutions from low-entropy to high-entropy alloys. *Curr Opin Solid State Mater Sci*. 2017;21(6):299–311.
[31] Maiti S, Steurer W. Structural-disorder and its effect on mechanical properties in single-phase TaNbHfZr high-entropy alloy. *Acta Mater*. 2016;106:87–97.
[32] Stepanov ND, Shaysultanov DG, Salishchev GA, et al. Structure and mechanical properties of a light-weight AlNbTiV high entropy alloy. *Mater Lett*. 2015;142:153–155.
[33] Jayaraj J, Thirathipviwat P, Han J, et al. Microstructure, mechanical and thermal oxidation behavior of AlNbTiZr high entropy alloy. *Intermetallics*. 2018;100:9–19.
[34] Wu YD, Cai YH, Wang T, et al. A refractory $Hf_{25}Nb_{25}Ti_{25}Zr_{25}$ high-entropy alloy with excellent structural stability and tensile properties. *Mater Lett*. 2014;130:277–280.
[35] Lee JH, Ha SV, Seong J, et al. Development of 3D interconnected nanoporous TiZrHfNbTaNi high-entropy alloy via liquid metal dealloying and subsequent synthesis of (TiZrHfNbTaNi)O high-entropy oxide. *J Mater Res Technol*. 2025;35:5204–5215.
[36] Sun J, Ning S, Zhao J, et al. High entropy cemented carbide coupling high entropy ceramic and high entropy alloy. *Appl Mat Today*. 2025;42:102563.
[37] Wang L, Zhang L, Lu X, et al. Surprising cocktail effect in high entropy alloys on catalyzing magnesium hydride for solid-state hydrogen storage. *Chem Eng J*. 2023;465:142766.
[38] Maddox J. New gas constant measurement. *Nature*. 1988;331(6156):477–477.
[39] Aamlid SS, Oudah M, Rottler J, et al. Understanding the role of entropy in high entropy oxides. *J Am Chem Soc*. 2023;145(11):5991–6006.
[40] El-Atwani O, Li N, Li M, et al. Outstanding radiation resistance of tungsten-based high-entropy alloys. *Sci Adv*. 2019;5(3):eaav2002.
[41] Dixit S, Rodriguez S, Jones MR, et al. Refractory high-entropy alloy coatings for high-temperature aerospace and energy applications. *J Therm Spray Technol*. 2022;31(4):1021–1031.
[42] Anand G, Goodall R, Freeman CL. Role of configurational entropy in body-centred cubic or face-centred cubic phase formation in high entropy alloys. *Scr Mater*. 2016;124:90–94.
[43] Li Z, Zhao S, Ritchie RO, et al. Mechanical properties of high-entropy alloys with emphasis on face-centered cubic alloys. *Prog Mater Sci*. 2019;102:296–345.
[44] Zhang Y, Ye S, Ke H, et al. In situ synthesis of N-containing CoCrFeNi high entropy alloys with enhanced properties fabricated by selective laser melting. *Mater Des*. 2023;229:111891.
[45] Li Z, Qiao D, Xu Y, et al. Cu-bearing high-entropy alloys with excellent antiviral properties. *J Mater Sci Technol*. 2021;84:59–64.
[46] Zhao C, Ding F, Lu Y, et al. High-entropy layered oxide cathodes for sodium-ion batteries. *Angew Chem*. 2019;132(1):270–275.
[47] Su H, Ma C, Zhou K, et al. Spinel high-entropy oxide with high-valence Mo for ultra-sensitive H_2S detection and safety warning of all-solid-state battery. *Chem Eng J*. 2025;509:161377.
[48] Kante MV, Weber ML, Ni S, et al. A high-entropy oxide as high-activity electrocatalyst for water oxidation. *ACS Nano*. 2023;17(6):5329–5339.
[49] Xu Y, Xu X, Bi L. A high-entropy spinel ceramic oxide as the cathode for proton-conducting solid oxide fuel cells. *J Adv Ceram*. 2022;11(5):794–804.
[50] Wang B, Wang Q, Sun B, et al. Nitride-reinforced HfNbTaTiV high-entropy alloy with excellent room and elevated-temperature mechanical properties. *J Mater Sci Technol*. 2023;149:31–41.
[51] Li J, Chen Y, Zhao Y, et al. Super-hard (MoSiTiVZr)Nx high-entropy nitride coatings. *J Alloys Compd*. 2022;926:166807.
[52] Wang F, Monteverde F, Cui B. Will high-entropy carbides and borides be enabling materials for extreme environments? *Int J Extreme Manuf*. 2023;5(2):022002.
[53] Xin X, Liu L, Liu Y, et al. Novel perovskite-spinel composite conductive ceramics for SOFC cathode contact layer. *Int J Hydrog Energy*. 2018;43(51):23036–23040.
[54] Chen L, Li B, Guo J, et al. High-entropy perovskite $RETa_3O_9$ ceramics for high-temperature environmental/thermal barrier coatings. *J Adv Ceram*. 2022;11(4):556–569.
[55] Ozdemir HC, Yagci MB, Bedir E, et al. Optimizing mechanical properties and Ag ion release rate of silver coatings deposited on ti-based high entropy alloys. *Surf Coat Technol*. 2023;455:129221.
[56] Gao J, Jin Y, Fan Y, et al. Fabricating antibacterial CoCrCuFeNi high-entropy alloy via selective laser melting and in-situ alloying. *J Mater Sci Technol*. 2022;102:159–165.
[57] Dąbrowa J, Zajusz M, Kucza W, et al. Demystifying the sluggish diffusion effect in high entropy alloys. *J Alloys Compd*. 2019;783:193–207.
[58] Chang C-C, Hsiao Y-T, Chen Y-L, et al. Lattice distortion or cocktail effect dominates the performance of tantalum-based high-entropy nitride coatings. *Appl Surf Sci*. 2022;577:151894.
[59] Wang Z, Fang Q, Li J, et al. Effect of lattice distortion on solid solution strengthening of BCC high-entropy alloys. *J Mater Sci Technol*. 2018;34(2):349–354.
[60] Kuang J, Zhang P, Wang Q, et al. Formation and oxidation behavior of refractory high-entropy silicide $(NbMoTaW)Si_2$ coating. *Corros Sci*. 2022;198:110134.
[61] Wang R, Tang Y, Li S, et al. Effect of lattice distortion on the diffusion behavior of high-entropy alloys. *J Alloys Compd*. 2020;825:154099.
[62] Wang R, Chen W, Zhong J, et al. Experimental and numerical studies on the sluggish diffusion in face centered cubic Co-Cr-Cu-Fe-Ni high-entropy alloys. *J Mater Sci Technol*. 2018;34(10):1791–1798.
[63] Yang T, Huang J, Hu S, et al. High-entropy FeCoNiCuRu solid solutions triggered cocktail effect to achieve fine-tuning adsorption energy for boosting nitrate electroreduction to ammonia. *Chem Eng J*. 2024;500:157426.
[64] Fu Y, Li J, Luo H, et al. Recent advances on environmental corrosion behavior and mechanism of high-entropy alloys. *J Mater Sci Technol*. 2021;80:217–233.
[65] An B, Yang M, Shang Y, et al. Broad-spectrum photothermal high-entropy alloy powders for efficient solar-driven antibacterial and dye degradation. *J Mater Chem A*. 2025;13(11):7999–8014.
[66] Zhang X, Huang X, Jiang L, et al. Surface microstructures and antimicrobial properties of copper plasma alloyed stainless steel. *Appl Surf Sci*. 2011;258(4):1399–1404.
[67] Huang Y, Gao Q, Li C, et al. Facile synthesis of Zn^{2+}-based hybrid nanoparticles as a new paradigm for the treatment of internal bacterial infections. *Adv Funct Mater*. 2021;32(15):2109011.
[68] Smith JL, Tran N, Song T, et al. Robust bulk micro-nano hierarchical copper structures possessing exceptional bactericidal efficacy. *Biomaterials*. 2022;280:121271.

[69] Bi X, Bai Q, Liang M, et al. Silver peroxide nanoparticles for combined antibacterial sonodynamic and photothermal therapy. *Small*. 2021;18(2):e2104160.
[70] Xu Z, Zhang C, Wang X, et al. Release strategies of silver ions from materials for bacterial killing. *ACS Appl Bio Mater*. 2021;4(5):3985–3999.
[71] Muharram RA, Kamadjaja D, Salsabilla SA, et al. Determination of minimum inhibitory concentration and minimum bactericidal concentration of silver ion against Staphylococcus aureus. *Int J Pharm Res*. 2020;12(03):1667–1671.
[72] Landeen LK, Yahya MT, Kutz SM, et al. Microbiological evaluation of copper: silver disinfection units for use in swimming pools. *Water Sci Technol*. 1989;21(3):267–270.
[73] Dasari S, Kombaiah B, Poplawsky JD, et al. Microstructural evolution in doped high entropy alloys NiCoFeCr-3X (X=Pd/Al/Cu) under irradiation. *J Nucl Mater*. 2024;598:155194.
[74] Yang C-M, Liu X-B, Liu Y-F, et al. Effect of Cu-doping on tribological properties of laser-cladded $FeCoCrNiCu_x$ high-entropy alloy coatings. *Tribol Int*. 2023;188:108868.
[75] Zemanate AM, Júnior AMJ, de Lima Andreani GF, et al. Corrosion behavior of $AlCoCrFeNi_x$ high entropy alloys. *Electrochim Acta*. 2023;441:141844.
[76] Gómez-Esparza CD, Peréz-Bustamante R, Alvarado-Orozco JM, et al. Microstructural evaluation and nanohardness of an AlCoCuCrFeNiTi high-entropy alloy. *Int J Miner Metall Mater*. 2019;26(5):634–641.
[77] Qin Y, Wang Y, Guan S, et al. High-pressure preparation of high-hardness $CoCrFeNiMo_{0.4}$ high-entropy alloy. *Int J Refract Met Hard Mater*. 2022;102:105718.
[78] Yang Y-F, Hu F, Xia T, et al. High entropy alloys: a review of preparation techniques, properties and industry applications. *J Alloys Compd*. 2025;1010:177691.
[79] Zhou E, Qiao D, Yang Y, et al. A novel Cu-bearing high-entropy alloy with significant antibacterial behavior against corrosive marine biofilms. *J Mater Sci Technol*. 2020;46:201–210.
[80] Ai Y, He M-Q, Sun H, et al. Ultra-small high-entropy alloy nanoparticles: efficient nanozyme for enhancing tumor photothermal therapy. *Adv Mater*. 2023;35(23):2302335.
[81] Li Y, Liao Y, Zhang J, et al. High-entropy-alloy nanoparticles with enhanced interband transitions for efficient photothermal conversion. *Angew Chem Int Ed Engl*. 2021;60(52):27113–27118.
[82] Yougbaré S, Mutalik C, Krisnawati DI, et al. Nanomaterials for the photothermal killing of bacteria. *Nanomaterials (Basel)*. 2020;10(6):1123.
[83] Liu H, Xing F, Zhou Y, et al. Nanomaterials-based photothermal therapies for antibacterial applications. *Mater Des*. 2023;233:112231.
[84] Feng Y, Yao H, Sun Z, et al. Optimized photothermal conversion ability through interband transitions in FeCoNiCrMn high-entropy-alloy nanoparticles. *ACS Appl Mater Interfaces*. 2024;16(31):41027–41035.
[85] Lian Z, Sakamoto M, Matsunaga H, et al. Near infrared light induced plasmonic hot hole transfer at a nano-heterointerface. *Nat Commun*. 2018;9(1):2314.
[86] Chae A, Jo S, Choi Y, et al. Enhanced photothermal bactericidal activity of chemically reduced graphene oxide stabilized by tripodal amphiphile. *Appl Surf Sci*. 2019;474:111–117.
[87] Wang L, Gao F, Wang A, et al. Defect-rich adhesive molybdenum disulfide/rGO vertical heterostructures with enhanced nanozyme activity for smart bacterial killing application. *Adv Mater*. 2020;32(48):2005423.
[88] He C-Y, Gao X-H, Yu D-M, et al. Scalable and highly efficient high temperature solar absorber coatings based on high entropy alloy nitride AlCrTaTiZrN with different antireflection layers. *J Mater Chem A*. 2021;9(10):6413–6422.
[89] Zou Y, Zhang Y, Yu Q, et al. Photothermal bactericidal surfaces: killing bacteria using light instead of biocides. *Biomater Sci*. 2021;9(1):10–22.
[90] Grisales MA, Gaitan GB, Chimá DM, et al. Development of a silver-doped high-entropy nitride coating: bactericidal and antiviral evaluation for biomedical applications. *ACS Appl Bio Mater*. 2025;8(4):3015–3027.
[91] Wang C, Yuan F, Yan Z, et al. High entropy 2D layered double hydroxide nanosheet toward cascaded nanozyme-initiated chemodynamic and immune synergistic therapy. *J Am Chem Soc*. 2024;147(1):136–148.
[92] Yang X, Feng J, Li Y, et al. PdMoPtCoNi high entropy nanoalloy with d electron self-complementation-induced multisite synergistic effect for efficient nanozyme catalysis. *Adv Sci*. 2024;11(38):e2406149.
[93] Ai Y, Wang Z, Shi W, et al. Atomic-Level high-entropy nanozymes enable remarkable endogenous targeted catalysis and enhancing tumor photothermal therapy. *Adv Mater*. 2025;37(33):2502322.
[94] Zhou J, Wang W, Zhang Q, et al. Oxygen-supplied mesoporous carbon nanoparticles for enhanced photothermal/photodynamic synergetic therapy against antibiotic-resistant bacterial infections. *Chem Sci*. 2022;13(23):6967–6981.
[95] Qiao Y, Xu Y, Liu X, et al. Microwave assisted antibacterial action of garcinia nanoparticles on gram-negative bacteria. *Nat Commun*. 2022;13(1):2461.
[96] Dai S, Ye R, Huang J, et al. Distinct lipid membrane interaction and uptake of differentially charged nanoplastics in bacteria. *J Nanobiotechnol*. 2022;20(1):191.
[97] Li Y, Yang L, Liao Y, et al. Photothermal heating-assisted superior antibacterial and antibiofilm activity of high-entropy-alloy nanoparticles. *Adv Funct Mater*. 2023;33(35):2302712.
[98] Gao Z, Zheng X, Dong X, et al. A general strategy for enhanced photodynamic antimicrobial therapy with perylenequinonoid photosensitizers using a macrocyclic supramolecular carrier. *Adv Healthc Mater*. 2024;13(28):2401778.
[99] Wu S, Xu C, Zhu Y, et al. Biofilm-sensitive photodynamic nanoparticles for enhanced penetration and antibacterial efficiency. *Adv Funct Mater*. 2021;31(33):2103591.
[100] Zhang M, Song Y, Wang J, et al. Enhancement effect of static magnetic field on bactericidal activity. *Small*. 2025;21(18):2412334.
[101] Huang Y, Chen X, Jiang Z, et al. Rare earth tungstate high-entropy ceramic powders containing holmium with broad-spectrum antibacterial and antiviral activity. *J Alloys Compd*. 2022;925:166721.
[102] Ren G, Huang L, Hu K, et al. Enhanced antibacterial behavior of a novel Cu-bearing high-entropy alloy. *J Mater Sci Technol*. 2022;117:158–166.
[103] Chen SY, Ding XW, Guo DX, et al. A novel low copper content antibacterial high-entropy alloy: role of synergistic effect of multiple elements. *J Mater Res Technol*. 2025;38:581–596.
[104] Zhou E, Yang Y, Li J, et al. A novel Cu and Ag bearing high-entropy alloy with remarkable antibacterial, antiviral and anti-microbial corrosion performances. *Adv Funct Mater*. 2024;35(15):2419467.
[105] Zhou E-Z, Ren G-Y, Sun Y-L, et al. Antibacterial activities of a novel Cu-bearing high-entropy alloy against multi-drug-resistant acinetobacter baumannii and Staphylococcus aureus. *Rare Met*. 2021;41(2):570–579.
[106] Wang P, You Q, Liu Y, et al. Combating infections from drug-resistant bacteria: unleashing synergistic broad-spectrum antibacterial power with high-entropy MXene/CDs. *Colloids Surf B Biointerfaces*. 2024;238:113874.
[107] Yadav A, Shinde PB, Mohan H, et al. Gut colonization with antibiotic-resistant Escherichia coli pathobionts leads to disease severity in ulcerative colitis. *Int J Antimicrob Agents*. 2024;64(4):107289.
[108] He B, Zhang F, Gong P, et al. An efficient, high-throughput enrichment system for the rapid detection of E. coli at low concentrations in water. *Anal Chim Acta*. 2025;1338:343571.
[109] Pan F, Altenried S, Scheibler S, et al. A rapid and specific antimicrobial resistance detection of Escherichia coli via magnetic nanoclusters. *Nanoscale*. 2024;16(6):3011–3023.
[110] Firyal S, Awan A, Khan A, et al. Public health hazard due to antibiotic resistant Staphylococcus aureus. *J Infect Public Health*. 2019;12(1):126.
[111] van Wamel WJB. Staphylococcus aureus infections, some second thoughts. *Curr Opin Infect Dis*. 2017;30(3):303–308.
[112] He X, Qian Y, Wu C, et al. Entropy-mediated high-entropy mxenes nanotherapeutics: NIR-II-enhanced intrinsic oxidase mimic activity to combat methicillin-resistant Staphylococcus aureus infection. *Adv Mater*. 2023;35(26):2211432.
[113] Wei Z, Xin F, Yang S, et al. Genetically engineered cell membrane modified conjugated polymer nanoparticles for NIR-II photothermal therapy. *Adv Mater Interfaces*. 2022;9(21):2200348.
[114] Gao J, Yuan L, Min Y, et al. D–A–D organic fluorescent probes for NIR-II fluorescence imaging and efficient photothermal therapy of breast cancer. *Biomater Sci*. 2024;12(5):1320–1331.
[115] Yao Z, Chen Y, Wang X, et al. High-entropy alloys catalyzing polymeric transformation of water pollutants with remarkably improved electron utilization efficiency. *Nat Commun*. 2025;16(1):148.
[116] Zhang Q, Qiu S, Wang L, et al. Multifunctional high-entropy alloys and oxides for self-powered electrocatalytic nitrate reduction to ammonia. *Chem Eur J*. 2025;31(24):e202500887.
[117] Lv ZY, Liu XJ, Jia B, et al. Development of a novel high-entropy alloy with eminent efficiency of degrading azo dye solutions. *Sci Rep*. 2016;6(1):34213.
[118] Liu Y, Liu H. Prediction of corrosion rates of a ship under the flow accelerated corrosion mechanism. *Corros Rev*. 2021;39(5):445–452.
[119] Esfidan MR, Ranji AR. Corrosion models for steel plates in ship structure based on statistical data. *Proc Inst Mech Eng Part M J Eng Marit Environ*. 2024;239(1):145–155.

[120] Choi YY, Lee SH, Park J-C, et al. The impact of corrosion on marine vapour recovery systems by voc generated from ships. *Int J Nav Archit Ocean Eng*. 2019;11(1):52–58.
[121] Wang J, Ding R, Li J, et al. Experimental study on microbial activity of ship ballast water and corrosion of ballast tank by inert flue gas deoxidation. *J Mater Eng Perform*. 2025;34(2):1560–1571.
[122] Soares CG, Garbatov Y, Zayed A, et al. Influence of environmental factors on corrosion of ship structures in marine atmosphere. *Corros Sci*. 2009;51(9):2014–2026.
[123] Ren H, Chen RR, Gao XF, et al. High-performance AlCoCrFeNi high entropy alloy with marine application perspective. *J Mater Res Technol*. 2023;25:6751–6763.
[124] Han S, Ma H, Chen H, et al. The wear, corrosion and antibacterial behaviors of $FeCrNiCuAl_x$ high-entropy alloy coatings prepared by laser cladding for marine applications. *J Mater Res Technol*. 2025;35:5034–5051.
[125] Verma A, Tarate P, Abhyankar AC, et al. High temperature wear in $CoCrFeNiCu_x$ high entropy alloys: the role of Cu. *Scr Mater*. 2019;161:28–31.
[126] Yu Y, Xu N, Zhu S, et al. A novel cu-doped high entropy alloy with excellent comprehensive performances for marine application. *J Mater Sci Technol*. 2021;69:48–59.
[127] Wang G, Xu J, Chen Y, et al. Assessment of the tribocorrosion performance of a (ZiZrNbTaMo)C refractory high entropy alloy carbide coating in a marine environment. *J Alloys Compd*. 2023;965:171342.
[128] Yaku K, Palikhe S, Iqbal T, et al. Nicotinamide riboside and nicotinamide mononucleotide facilitate NAD synthesis via enterohepatic circulation. *Sci Adv*. 2025;11(12):1538.
[129] Zhang M, Jia H, Zhuang L, et al. Ultrathin high-entropy hydrotalcites-based injectable hydrogel with programmed bactericidal and anti-inflammatory effects to accelerate drug-resistant bacterial infected wound healing. *Colloids Surf B Biointerfaces*. 2025;247:114450.
[130] Li S, Yang C, Li J, et al. Progress in pluronic f127 derivatives for application in wound healing and repair. *Int J Nanomedicine*. 2023;18:4485–4505.
[131] Yang L, Zhou E, Dong Y, et al. Al/Cu enhancement in marine antibiofouling and anti-biocorrosion performance of high-entropy alloys. *Adv Funct Mater*. 2025;21:2502816.
[132] Yu M, Qiu Y, Wang Y, et al. Engineering multifunctional high-entropy oxide nanozymes for robust marine antifouling. *J Colloid Interface Sci*. 2025;693:137604.
[133] Wang J, Diao W, Cheng B, et al. Excellent tribocorrosion resistance in artificial seawater of high entropy alloy FeCrNiCoAl coating prepared by HOVF. *J Alloys Compd*. 2024;1009:176931.
[134] Ma X, Ren P, Zhang S, et al. A significant improvement in corrosion resistance and biocompatibility in ZrNbTiCrCu high-entropy films induced by the precipitation of cu. *J Mater Sci Technol*. 2025;219:213–224.
[135] Zhu X, Wang J, Du Y, et al. Gallium containing high entropy alloy inhibits biofilm formation and enhances osseointegration. *Compos Part B*. 2025;295:112194.
[136] Luo T, Shi Y, Liang T, et al. Low elastic modulus and superb antibacterial performance in copper-bearing refractory high-entropy alloys. *J Alloys Compd*. 2025;1026:180352.
[137] Yu B, Juma T, Wang H, et al. Development of new $Ti_{50}Zr_{25}Nb_{20}Cu_5$–Ag high-entropy alloys with excellent antibacterial property, osteoconductivity and biocompatibility in vitro and in vivo. *J Mater Sci Technol*. 2023;141:209–220.
[138] Zhou Y, Shen X, Qian T, et al. A review on the rational design and fabrication of nanosized high-entropy materials. *Nano Res*. 2023;16(5):7874–7905.
[139] Iijima Y, Nagase T, Matsugaki A, et al. Design and development of Ti-Zr-Hf Nb-Ta-Mo high-entropy alloys for metallic biomaterials. *Mater Des*. 2021;202:109548.
[140] Medina LZ, Mølmen L, Paschalidou E-M, et al. Extending the passive region of CrFeNi-based high entropy alloys. *Adv Funct Mater*. 2023;33(51):2307897.
[141] Jia Y-J, Chen H-N, Liang X-D. Microstructure and wear resistance of CoCrNbNiW high-entropy alloy coating prepared by laser melting deposition. *Rare Met*. 2019;38(12):1153–1159.
[142] Yang JX, Dai B-H, Chiang C-Y, et al. Rapid fabrication of high-entropy ceramic nanomaterials for catalytic reactions. *ACS Nano*. 2021;15(7):12324–12333.
[143] Yin S, Li W, Song B, et al. Deposition of FeCoNiCrMn high entropy alloy (HEA) coating via cold spraying. *J Mater Sci Technol*. 2019;35(6):1003–1007.
[144] Tian Y-Z, Peng S-Y, Chen S-F, et al. Temperature-dependent tensile properties of ultrafine-grained C-doped CoCrFeMnNi high-entropy alloy. *Rare Met*. 2022;41(8):2877–2885.
[145] Bajaj D, Feng A, Qu S, et al. Deformation behavior of 3D-printed high-entropy alloys: a critical review. *Adv Eng Mater*. 2023;26(4):2300615.
[146] Ma J, Huang C. High entropy energy storage materials: synthesis and application. *J Storage Mater*. 2023;66:107419.

How to cite this article: Xue P-W, Chang Y-L, Wang C, Sun G-T, Gao R-T, He C-Y, Gao X-H. High-entropy antibacterial materials. MedMat 2026;3(1):e00026. doi: 10.1097/mm9.0000000000000026